

# Conserved V-ATPase c subunit plays a role in plant growth by influencing V-ATPase-dependent endosomal trafficking

Aimin Zhou<sup>1</sup>, Yuanyuan Bu<sup>1</sup>, Tetsuo Takano<sup>2</sup>, Xinxin Zhang<sup>1</sup> and Shenkui Liu<sup>1,\*</sup>

<sup>1</sup>Key Laboratory of Saline-alkali Vegetation Ecology Restoration in Oil Field (SAVER), Ministry of Education, Alkali Soil Natural Environmental Science Center (ASNES), Northeast Forestry University, Harbin, China

<sup>2</sup>Asian Natural Environmental Science Center, The University of Tokyo, Nishitokyo-shi, Tokyo, Japan

Received 30 September 2014;

revised 10 March 2015;

accepted 18 March 2015.

\*Correspondence (Tel/Fax

+86 451 82191394; email shenkui@nefu.edu.cn)

## Summary

In plant cells, the vacuolar-type H<sup>+</sup>-ATPases (V-ATPase) are localized in the tonoplast, Golgi, trans-Golgi network and endosome. However, little is known about how V-ATPase influences plant growth, particularly with regard to the V-ATPase c subunit (VHA-c). Here, we characterized the function of a VHA-c gene from *Puccinellia tenuiflora* (PutVHA-c) in plant growth. Compared to the wild-type, transgenic plants overexpressing PutVHA-c in *Arabidopsis thaliana* exhibit better growth phenotypes in root length, fresh weight, plant height and silique number under the normal and salt stress conditions due to noticeably higher V-ATPase activity. Consistently, the *Arabidopsis atvha-c5* mutant shows reduced V-ATPase activity and retarded plant growth. Furthermore, confocal and immunogold electron microscopy assays demonstrate that PutVHA-c is mainly localized to endosomal compartments. The treatment of concanamycin A (ConcA), a specific inhibitor of V-ATPases, leads to obvious aggregation of the endosomal compartments labelled with PutVHA-c-GFP. Moreover, ConcA treatment results in the abnormal localization of two plasma membrane (PM) marker proteins Pinformed 1 (AtPIN1) and regulator of G protein signalling-1 (AtRGS1). These findings suggest that the decrease in V-ATPase activity blocks endosomal trafficking. Taken together, our results strongly suggest that the PutVHA-c plays an important role in plant growth by influencing V-ATPase-dependent endosomal trafficking.

**Keywords:** *Puccinellia tenuiflora*, V-ATPase c subunit (VHA-c), activity, concanamycin A, endosomal trafficking, *Arabidopsis thaliana*.

## Introduction

Vacuolar-type H<sup>+</sup>-ATPases (V-ATPase) are multisubunit endomembrane proton pumps that are highly conserved in eukaryotes. These pumps play important roles in various biological processes, including vesicle trafficking, ion homeostasis and protein degradation (Forgac, 2007; Marshansky and Futai, 2008). In plants, V-ATPases are localized in the tonoplast and the membranes of the secretory system such as the endoplasmic reticulum (ER), Golgi, small vesicles and provacuoles (Dettmer *et al.*, 2006; Herman *et al.*, 1994; Krebs *et al.*, 2010; Matsuoka *et al.*, 1997; Schumacher and Krebs, 2010; Sze *et al.*, 2002). V-ATPases consist of the cytosolic ATP-hydrolysing V<sub>1</sub> complex (subunits A to H) and the membrane-bound proton-translocating V<sub>0</sub> complex (subunits a, c, c', c'', d and e). The symmetrical arrangement of four or five copies of the V-ATPase c subunits (VHA-c) forms the core of the V<sub>0</sub> complex. VHA-c contains four putative transmembrane domains (TM1 to TM4), which represent approximately half of the VHA-c amino acids. The highly conserved Glu residue in TM4 acts as the proton-binding site (Hirata *et al.*, 2003; Nishi and Forgac, 2002). In yeast, VHA-c is encoded by a single-gene *Vma3*. The destruction of *Vma3* or the replacement of its TM4 Glu residue by a certain amino acid (such as Gln, Val or Lys) results in the loss of V-ATPase activity, suggesting that the functionality of V-ATPase depends on VHA-c (Noumi *et al.*, 1991; Umemoto *et al.*, 1990). concanamycin A (ConcA) is a membrane-permeable macrolide antibiotic that specifically binds to VHA-c and inhibits proton transport (Bowman *et al.*, 2004; Huss *et al.*, 2002).

In *Arabidopsis thaliana*, VHA-c is encoded by a multigene family comprising of five members (*AtVHA-c1*–*AtVHA-c5*), which display very high amino acid sequence identity (>98%) (Perera *et al.*, 1995; Sze *et al.*, 2002). Among them, *AtVHA-c1*, *AtVHA-c3* and *AtVHA-c5* have the identical amino acid sequence, but *AtVHA-c1* and *AtVHA-c3* are expressed in different tissues. *AtVHA-c1* is expressed mainly in cotyledons, hypocotyls and root elongation zone, whereas *AtVHA-c3* is expressed in the root cap, suggesting that the roles of *AtVHA-c* genes depend on their expression in specific organs and cell types (Padmanaban *et al.*, 2004). In addition, knock-down of either *AtVHA-c1* or *AtVHA-c3* decreases V-ATPase activity and impairs root growth in *Arabidopsis* (Padmanaban *et al.*, 2004).

VHA-c genes have been cloned from several plant species, including *Mesembryanthemum crystallinum* (Tsiantis *et al.*, 1996), *Pennisetum glaucum* (Tyagi *et al.*, 2005) and *Tamarix hispida* (Gao *et al.*, 2011). Based on these advances, we now know more about the characterization of VHA-c expression. For instance, Seidel *et al.* (2004) reported that a VHA-c from the *M. crystallinum* was localized in the endomembrane system and interacted with the VHA-a in plant cells. In addition, previous research also demonstrated that environmental stresses affect VHA-c gene expression. For instance, salt stress induces the expression of VHA-c in *M. crystallinum* (Löw *et al.*, 1996; Tsiantis *et al.*, 1996). Salinity and drought stresses also increase the abundance of VHA-c transcripts in *P. glaucum* (Tyagi *et al.*, 2005). Finally, overexpression of halophyte grass (*Spartina alterniflora* L.) VHA-c in rice enhances the salt tolerance (Baisakh *et al.*, 2012). To date, however, little information is available

about the function of VHA-c in plant growth, development and responses to stresses.

*Puccinellia tenuiflora* is a monocotyledonous halophyte species that thrives in the saline-alkaline soil of the Songnen plain in north-east China. Saline-alkaline soils are characterized by high salt content and the scarcity of free water and nutrition, and these extreme conditions directly limit crop growth. In this study, we characterized a VHA-c gene (*PutVHA-c*) from *P. tenuiflora*. The subcellular localization of PutVHA-c in plant cells was examined using GFP tagging, endosomal marker FM4-64 staining and immunogold electron microscopy. Furthermore, the contribution of *PutVHA-c* to V-ATPase activity and plant growth was investigated by genetic and pharmaceutical approaches in *Arabidopsis*.

## Results

### PutVHA-c is highly conserved and broadly expressed in plant tissues

The 872-bp full-length cDNA of *PutVHA-c* contains a 495-bp open reading frame (ORF). The deduced amino acid sequence of PutVHA-c is highly similar to that of VHA-c proteins from other plant species (>98.3 identities), including *Arabidopsis thaliana*, *Oryza sativa*, *Zea mays* and *Brachypodium distachyon* (Figure S1a). Similar to other VHA-c proteins, PutVHA-c has four putative transmembrane domains (Figure S1b), with a conserved Glu residue in the fourth transmembrane domain (Figure S1a). In *Arabidopsis*, the VHA-c family consists of three highly conserved members, which are encoded by five different genes (*AtVHA-c1~c5*). Among them, amino acid sequences of *AtVHA-c1*, *AtVHA-c3* and *AtVHA-c5* are identical (named *AtVHA-c1*, 3, 5) (Figure S2). Remarkably, PutVHA-c displayed very high amino acid sequence identity (>97.8%) with *AtVHA-c* proteins. These results indicate that VHA-c is extremely conserved in plant species.

To dissect the biological functions of VHA-c, we firstly investigated its expression patterns in various organs and in response to abiotic stress. The semiquantitative PCR analysis (method is described in the Data S1) showed that *PutVHA-c* was expressed in all tissues of *P. tenuiflora*, with relatively higher expression levels in the leaf, sheath and anther (Figure 1a). Northern blot analysis (Data S1) revealed that *PutVHA-c* expression was induced dramatically by NaCl (200 mM) but slightly by Na<sub>2</sub>CO<sub>3</sub> (20 mM) or NaHCO<sub>3</sub> (100 mM) in *P. tenuiflora* leaves and roots after 12 or 24 h of treatment (Figure 1b). To get better understanding of VHA-c expression profiles, we then investigated the abiotic stress-induced expression and tissue expression specificity of *AtVHA-c1~c5* genes in *Arabidopsis*. Expectedly, real-time quantitative PCR analysis (Data S1) showed that expression of *AtVHA-c1~c5* genes was strongly and differentially induced by NaCl (150 mM), mannitol (250 mM), H<sub>2</sub>O<sub>2</sub> (5 mM), low nutrition (agar) and cold (4 °C) (Figure 1c–g). These results suggest that VHA-c is involved in plant responses to multiple abiotic stimuli. Because the *AtVHA-c* proteins are extremely conserved, differential expression patterns are usually used to examine their functions (Padmanaban *et al.*, 2004). Here, we checked the gene expression of *AtVHA-c1~c5* in different tissues of *Arabidopsis* by monitoring promoter-driven β-glucuronidase (GUS) activity (Data S1). *AtVHA-c1~c5* were indeed expressed in different tissues (Figure 2). Among the five genes, *AtVHA-c1/4/5* exhibited relatively higher expression levels than *AtVHA-c2/3* in leaf (Figure 2, fourth column) and flower tissues (Figure 2, fifth column). However, all five genes appear to be expressed at the

same levels in the anther tissues (Figure 2, sixth column). These results suggest that the expression of VHA-c genes is regulated in a tissue-specific manner.

### Phenotypic analysis of transgenic *Arabidopsis* plants overexpressing *PutVHA-c*

To explore the physiological function of *PutVHA-c*, we generated transgenic *Arabidopsis* plants expressing *PutVHA-c* under the control of the CaMV35S promoter. The expression of *PutVHA-c* in the transgenic lines was confirmed by northern blotting (Figure 3a). We firstly compared the phenotype of the wild-type (WT) and transgenic plants under normal cultural conditions. As shown in Figure 3b, at the early seedling stage, transgenic plants displayed longer primary roots on the 1/2 MS medium than WT. Statistical analysis revealed that 10-day-old transgenic seedlings produced 40%–56% longer length of roots (Figure 3c) and had 28%–33% higher fresh weight (Figure 3d) than WT. Furthermore, at the vegetative stage, 30-day-old soil-grown transgenic plants displayed more rosette leaves than WT (Figure 3e,f). Notably, transgenic plants flowered earlier than WT (Figure 3g). At the reproductive stage, mature transgenic plants also exhibited more inflorescence stems and siliques (Figure 3h), as well as larger seeds than WT (Figure S3a–c). These results indicate that overexpression of *PutVHA-c* in *Arabidopsis* promotes plant growth and development and ultimately increases seed yield under normal cultural conditions.

Considering the high sequence identity of PutVHA-c and *AtVHA-c* proteins (Figure S2), we hypothesized that they might play similar roles in plant growth. To test this hypothesis, we overexpressed *AtVHA-c3* in *Arabidopsis*. Compared with WT plants, *AtVHA-c3* transgenic *Arabidopsis* plants also had more inflorescence stems and rosette leaves, and larger seeds than WT (Figure S4a–d). These phenotypes were similar to those observed in transgenic plants overexpressing *PutVHA-c* (Figure 3f–h). Taken together, our data suggest that VHA-c plays an important role in the regulation of plant growth and development.

The above data prompted us to investigate whether the better growth of transgenic plants is related to an increase in V-ATPase activity. We found that V-ATPase activity in the transgenic plants was enhanced by 31%–48% compared with that in WT (Table 1). To further confirm the relationship between V-ATPase activity and plant growth, we used an inhibitor concanamycin A (ConcA) of V-ATPase activity (Huss *et al.*, 2002). ConcA treatment severely inhibited root growth of both WT and *PutVHA-c* transgenic seedlings (Figure S5). The difference in root growth between WT and transgenic seedlings gradually decreased and even disappeared with the increase of the ConcA concentration (Figure S5). These results support the idea that *PutVHA-c* overexpression promotes plant growth by increasing the V-ATPase activity in *Arabidopsis*.

Because a complete knockout of *AtVHA-c* genes is likely to be lethal (Padmanaban *et al.*, 2004; Schumacher *et al.*, 1999), we only identified a *atvha-c5* mutant, which held a T-DNA insertion in the 3' untranslated region of the *AtVHA-c5* gene (Figure 4a). Real-time quantitative PCR analysis revealed that the *AtVHA-c5* mRNA level in *atvha-c5* was approximately 20% of that in WT (Figure 4b). The V-ATPase activity in *atvha-c5* was approximately 70% of that in WT (Figure 4c). Finally, we observed that *atvha-c5* exhibited shorter primary roots and less biomass accumulation than WT when grown on the 1/2 MS medium, as evidenced by the quantitative assays of root length and fresh weight (Figure 4d–f). Taken altogether, these results demonstrate the

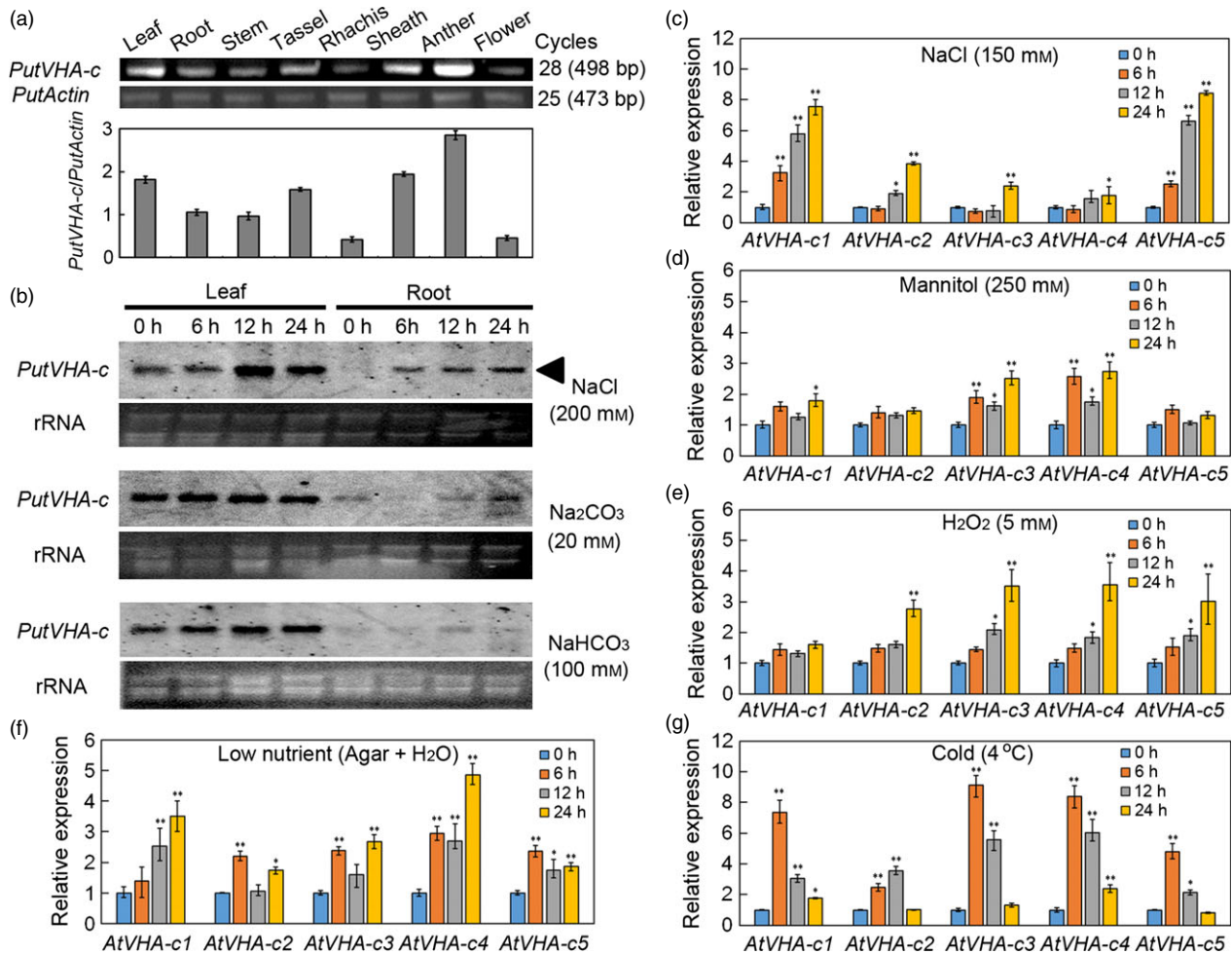


**Figure 1** Expression analysis of *VHA-c* genes from *Puccinellia tenuiflora* and *Arabidopsis*. (a) Semiquantitative PCR (upper) and quantitative (below) analysis of *PutVHA-c* in different organs of *P. tenuiflora*; (b) northern blot analysis of the expression of *P. tenuiflora PutVHA-c* in response to NaCl, Na<sub>2</sub>CO<sub>3</sub> and NaHCO<sub>3</sub> stresses. Total RNA was isolated from the leaves and roots of 2-week-old *P. tenuiflora* plants treated with 200 mM NaCl, 20 mM Na<sub>2</sub>CO<sub>3</sub> or 100 mM NaHCO<sub>3</sub> for 0, 6, 12 and 24 h; (c–g) real-time quantitative analysis of the expression of *Arabidopsis AtVHA-c1-5* genes in response to various abiotic stresses. Ten-day-old *Arabidopsis* seedlings were treated with 150 mM NaCl (c), 250 mM mannitol (d), 5 mM H<sub>2</sub>O<sub>2</sub> (e), low nutrient levels (f) or stored at 4 °C (g) for 0, 6, 12 and 24 h. The *AtActin2* gene was used as an internal control, and the transcript level in untreated seedlings was set as 1.0. Asterisks indicate a significant difference between untreated and stress-treated seedlings (\**P* < 0.05; \*\**P* < 0.01). Error bars represent SD (*n* = 3).

involvement of *AtVHA-c5* in regulating plant growth and further suggest that *VHA-c* positively affects plant growth by influencing V-ATPase activity.

As *PutVHA-c* expression is induced by NaCl stress (Figure 1b), we then investigated the influence of *PutVHA-c* overexpression on plant tolerance to NaCl stress. Prior to conducting the NaCl tolerance test, we ascertained that WT and transgenic lines exhibit similar growth under 1/8 MS medium (Figure 5a). Next, root length assays showed that transgenic seedlings exhibited longer roots on both 1/2 MS and 1/8 MS media supplemented with either 75 or 100 mM NaCl (Figure 5b,c). Additionally, a relative root length analysis showed that root growth of transgenic seedlings was less inhibited by NaCl stress compared with the WT (Figure 5b,c). We further applied the noninvasive ion-selective microelectrode technique (NMT) (Data S1) to determine Na<sup>+</sup> movement in the roots of WT and transgenic seedlings precultured on media containing either 10 or 50 mM NaCl for 24 h. We observed that Na<sup>+</sup> efflux in the transgenic seedling roots was higher than efflux in the WT seedling roots (Figure S6a–

c), implying that *PutVHA-c* overexpression plays a role in Na<sup>+</sup> efflux. In sum, these results indicate that the overexpression of *PutVHA-c* in *Arabidopsis* can alleviate the inhibition of NaCl stress on plant root growth.

#### PutVHA-c is mainly localized to endosomal compartments

We examined the subcellular localization of *PutVHA-c* in plant cells, which is critical for a full functional analysis. First, green fluorescent protein (GFP)-fused *PutVHA-c* (*PutVHA-c*-GFP) was expressed in *P. tenuiflora* suspension cells using *Agrobacterium*-mediated transformation (Data S1). Confocal scanning revealed that *PutVHA-c*-GFP was detected in the punctate structures of *P. tenuiflora* suspension cells (Figure 6a). To confirm this result, we then generated transgenic *Arabidopsis* plants stably expressing the *PutVHA-c*-GFP. In agreement with the above result, the fluorescence of *PutVHA-c*-GFP was detected in the punctate structures in leaf, hypocotyl and root epidermal cells of the transgenic plants (Figure 6b). However, we observed that

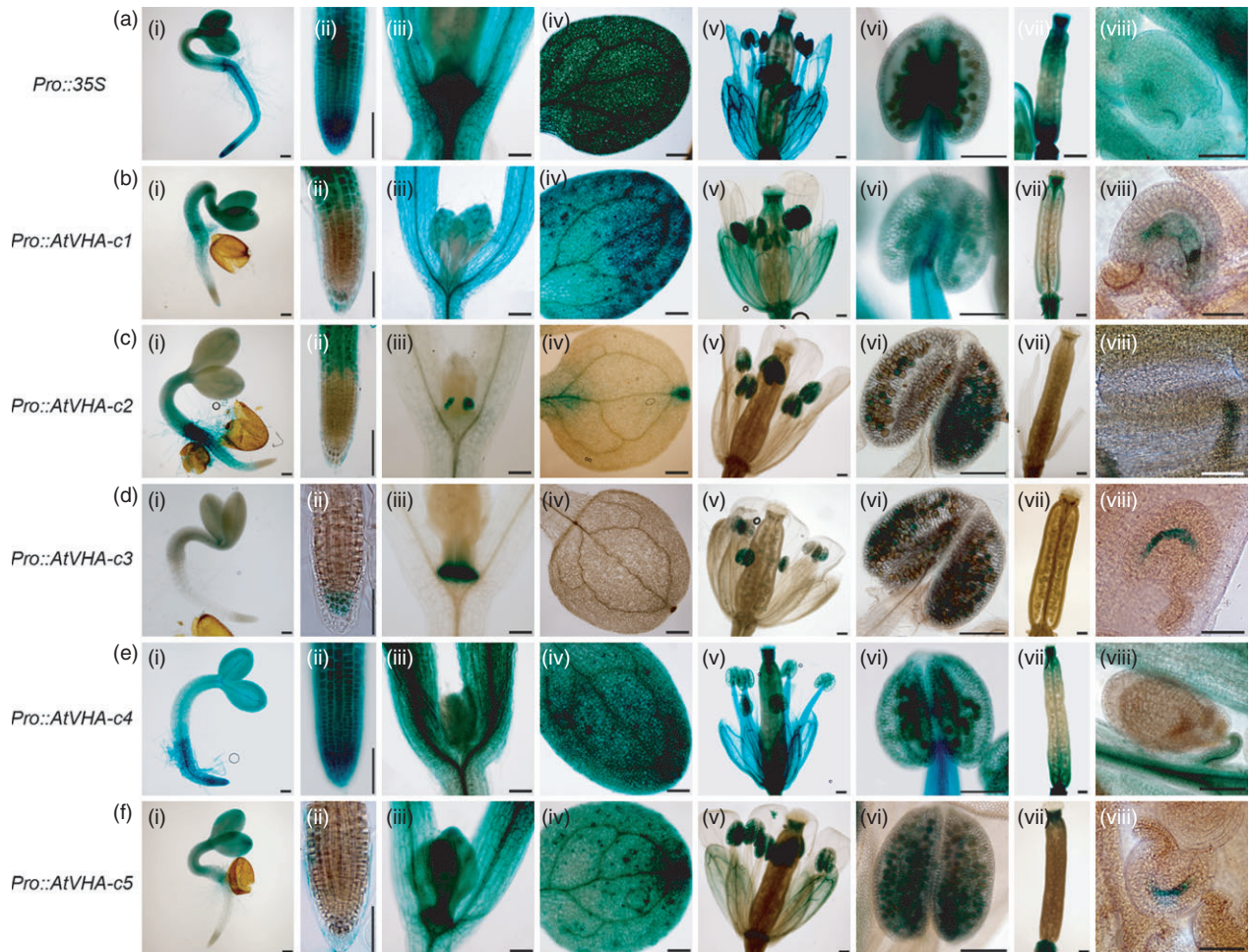


**Figure 2** *AtVHA-c1-c5* genes promoter-GUS expression in transgenic *Arabidopsis*. Histochemical GUS staining was carried out at different stages of development and in various tissues of *AtVHA-c1-c5* genes promoter-GUS transgenic *Arabidopsis* plants. (a) *Pro35S::GUS* expression in all tissues; (b) *ProAtVHA-c1::GUS* expression in all tissues of the seedlings except the root meristematic zone (ii), sepal (v), stamen, anther (vi), silique (vii) and embryo sac (viii); (c) *ProAtVHA-c2::GUS* expression in the root maturation zone (i, ii), stipules (iii), cotyledon apex (iv), pollen grains (vi) and funicle (viii); (d) *ProAtVHA-c3::GUS* expression in the root meristematic zone (ii), base of the leaves (iii), pollen grains (vi) and embryo sac (viii); (e) *ProAtVHA-c4::GUS* expression in all tissues of the seedlings (i–iv), flower (v), stamen (vi), silique (vii) and funicle (viii); (f) *ProAtVHA-c5::GUS* expression in the leaf (i, iii and iv), the root epidermal cells (ii), sepals (v), pollen grains (vi), top and base of the silique (vii) and embryo sac (viii). Scale bar = 200  $\mu$ m.

the PutVHA-c-GFP-localized compartment was different from the Golgi (GmMan1-YFP) (Hu *et al.*, 2013), tonoplast (At $\gamma$ TIP-GFP) (Sun *et al.*, 2012) and plasma membrane (PM) (AtRGS1-GFP) (Hu *et al.*, 2013) markers in root cells (Figure S7a–e). In protoplasts isolated from mesophyll cells of transgenic *Arabidopsis*, PutVHA-c-GFP was detected in the punctate structures (Figure 7b). In addition, fluorescence of AtVHA-c3-GFP in *Arabidopsis* mesophyll protoplasts was also detected in the punctate structures (Figure S8). To test whether the PutVHA-c-GFP-localized compartment is an endosomal compartment, the localization of PutVHA-c-GFP was compared with that of the endosomal marker dye FM4-64. FM4-64 is widely considered to follow the endocytic pathway, from the PM via endosomes to the tonoplast (Bolte *et al.*, 2004; Ueda *et al.*, 2001) (Figure S9 and S10). After FM4-64 staining, PutVHA-c-GFP was colocalized with FM4-64 in different-sized endosomal compartments (Figure 7c–f), which were distributed in the cytoplasm (Figure 7c), and close to the PM (Figure 7e) or central vacuole (Figure 7d,f).

Immunogold electron microscopy (IEM) was further performed to confirm the localization of PutVHA-c-GFP. In ultrathin cryo-

sections of the leaf probed with a GFP antibody, gold particles were specifically associated with the endosomal membrane (Figure 8a,b). Furthermore, gold particles were also observed in different-sized endosomal membranes in the cytoplasm (Figure 8c), and close to the central vacuole (Figure 8d) or PM (Figure 8e). Moreover, PutVHA-c-GFP overlapped partially with the PM as short lines (Figure S11a–c), and gold particles were also detected on the PM (Figure S11d,e). These results indicate that PutVHA-c is mainly localized to endosomal compartments and is likely to be distributed throughout the secretory pathway.

#### ConcA perturbs endosomal trafficking and the sorting of PM proteins AtPIN1 or AtRGS1

Next, we pretreated PutVHA-c-GFP-expressing root cells with ConcA to inhibit the secretory pathway. Previous studies have shown that ConcA blocks all post-Golgi trafficking (Cai *et al.*, 2011; Reichardt *et al.*, 2007; Robinson *et al.*, 2008; Viotti *et al.*, 2010). First, we treated the root cells of WT with ConcA. Treatment with ConcA caused the aggregation of the large vesicular structure in the vicinity of Golgi stacks in the WT root

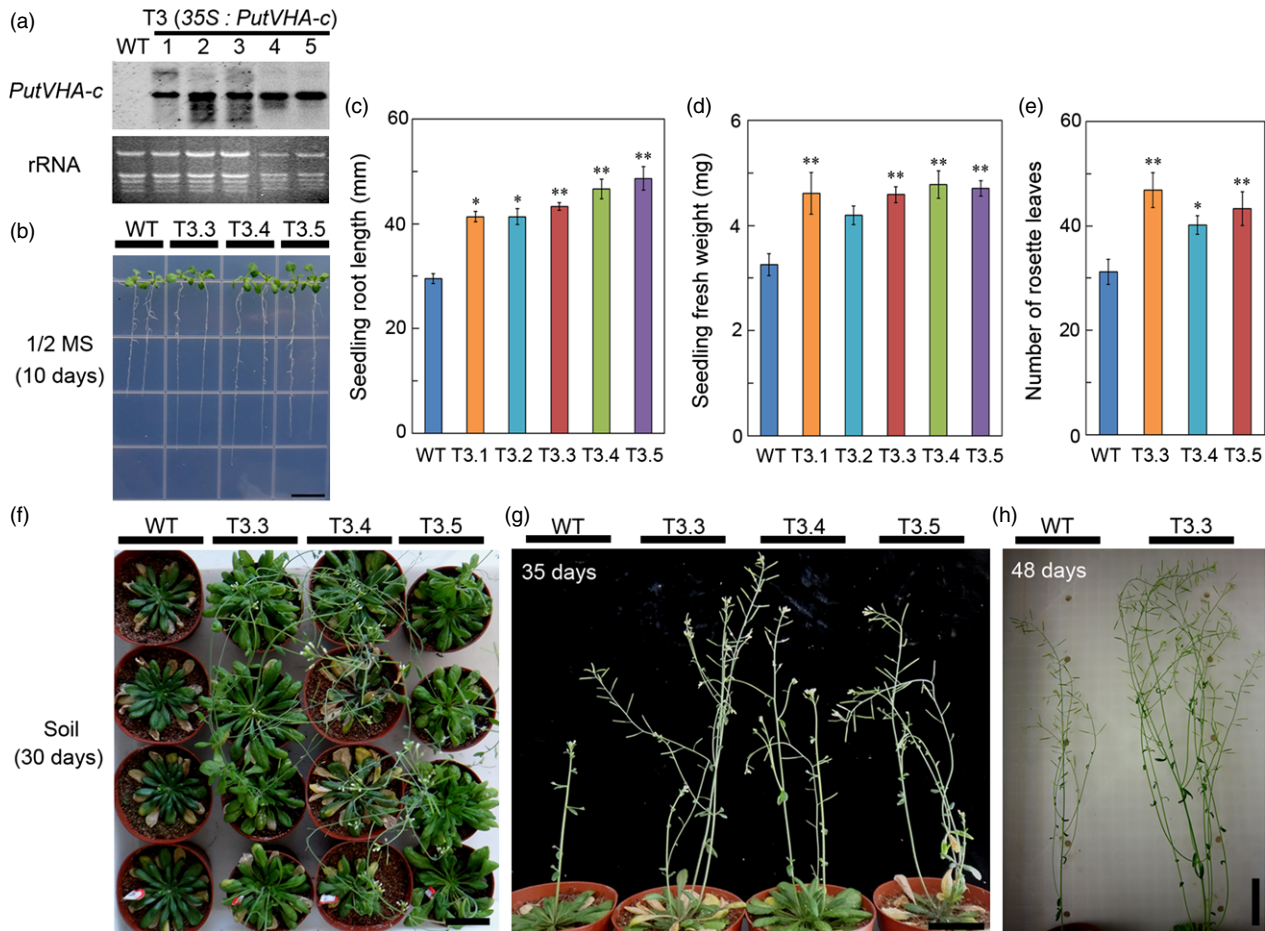


**Figure 3** Phenotypes of wild-type (WT) and transgenic *Arabidopsis* plants overexpressing *PutVHA-c*. (a) Northern blot analysis of transgenic *Arabidopsis* lines (T3.1–T3.5); (b–d) phenotypes of WT and transgenic seedlings (10-day-old) on vertical plates containing 1/2 MS (b), their root lengths (c) and fresh weights (d). Error bars represent SE ( $n = 15$ ); (e and f) number (e) and phenotypes (f) of rosette leaves of WT and transgenic plants (T3.3–T3.5) grown on soil for 30 days. Seedlings were germinated and grown on 1/2 MS medium for 10 days before being transferred to soil; (g and h) phenotypes of WT and transgenic plants (T3.3–T3.5) grown on soil for 35 (g) or 48 days (h). Asterisks indicate a significant difference between WT and transgenic plants ( $*P < 0.05$ ;  $**P < 0.01$ ). Scale bars = 1 cm (b), 5 cm (f–h).

**Table 1** Analysis of V-ATPase activity in wild-type (WT) and transgenic *Arabidopsis* seedlings (T3.3–T3.5). Microsomal proteins were prepared from 14-day-old seedlings grown on 1/2 MS plates, and their V-ATPase activity was measured by monitoring the oxidation of NADH. Data from at least three independent measurements were averaged

Plant lines	V-ATPase activity (NADH $\mu\text{mol min}^{-1} \text{mg} \pm \text{SE}$ )	Average, %
WT	$0.90 \pm 0.17$	100
T3.3	$1.34 \pm 0.10^{**}$	148
T3.4	$1.18 \pm 0.15^*$	131
T3.5	$1.21 \pm 0.13^*$	134

Asterisks indicate a significant difference between WT and transgenic plants ( $*P < 0.05$ ;  $**P < 0.01$ ).

cells (Figure 9b). In response to this treatment, ConcA caused the aggregation of PutVHA-c-GFP-labelled endosomal compartments in the root cells of *PutVHA-c-GFP* transgenic seedlings (Figure 9d). These results suggest that (i) the reduction of V-ATPase activity by ConcA interfered with endosomal trafficking,

and (ii) PutVHA-c-GFP-labelled endosomal compartments may derive from the Golgi apparatus and are distributed throughout the secretory pathway. Endosomes of the secretory pathway are responsible for the transport of newly synthesized proteins from the endoplasmic reticulum (ER) to their destinations via the Golgi apparatus (Bassham *et al.*, 2008; Contento and Bassham, 2012; Richter *et al.*, 2009; Robinson *et al.*, 2012). Therefore, we further investigated whether V-ATPase activity affects the secretory trafficking using two PM marker proteins, the auxin efflux carrier Pinformed 1 (AtPIN1) (Geldner *et al.*, 2001) and the regulator of G protein signalling-1 (AtRGS1) (Hu *et al.*, 2013). Both AtPIN1 and AtRGS1 are involved in aspects of plant growth and development (Chen *et al.*, 2003; Krecek *et al.*, 2009; Urano *et al.*, 2012). In the root cells of untreated *Arabidopsis* seedlings, AtPIN1-GFP and AtRGS1-GFP were detected only in the PM (Figure 9e,g), whereas seedlings treated with ConcA showed increased intracellular GFP signals in irregular patches (Figure 9f,h). In contrast, ConcA treatment did not change the distribution of GFP protein expressed alone, which was used as a control (Figure 9i,j). These results indicate that AtPIN1 or AtRGS1 trafficking to the PM is dependent on V-ATPase activity. Taken together, these data suggest that

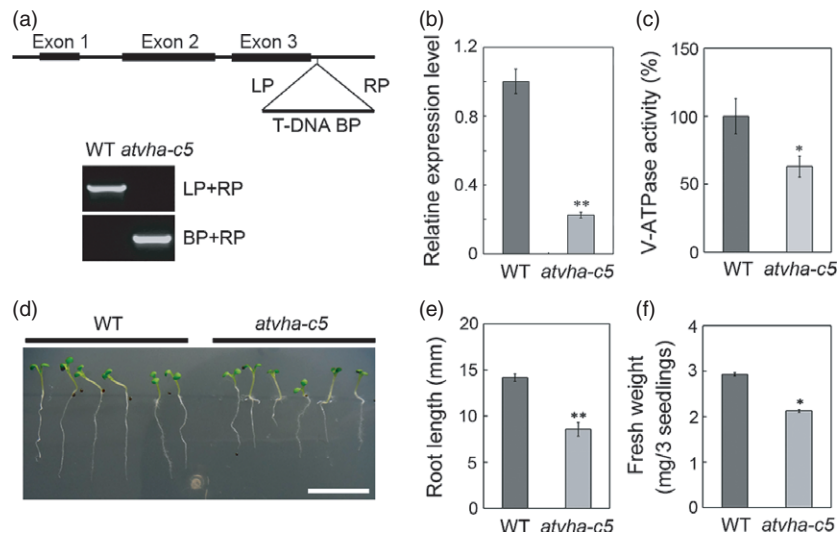


**Figure 4** Phenotypic characterization and V-ATPase activity analysis in the *Arabidopsis atvha-c5* mutant. (a and b) Schematic representation of the *AtVHA-c5* gene and the position of the T-DNA insertion (a, upper). Genotyping (Genomic DNA) and relative expression (mRNA) analysis of *AtVHA-c5* in the *atvha-c5* mutant using PCR (a, below) and real-time quantitative PCR (b), respectively; (c) V-ATPase activity analysis in the WT and *atvha-c5* mutant. Error bars indicate the SE ( $n = 3$ ); (d–f) phenotypes of WT and transgenic seedlings (5-day-old) on vertical plates containing 1/2 MS (d), their root lengths (e) and fresh weights (f). Error bars indicate the SE ( $n = 9$ ). Asterisks indicate a significant difference between WT and mutant plants ( $*P < 0.05$ ;  $**P < 0.01$ ). Scale bar = 1 cm (d).

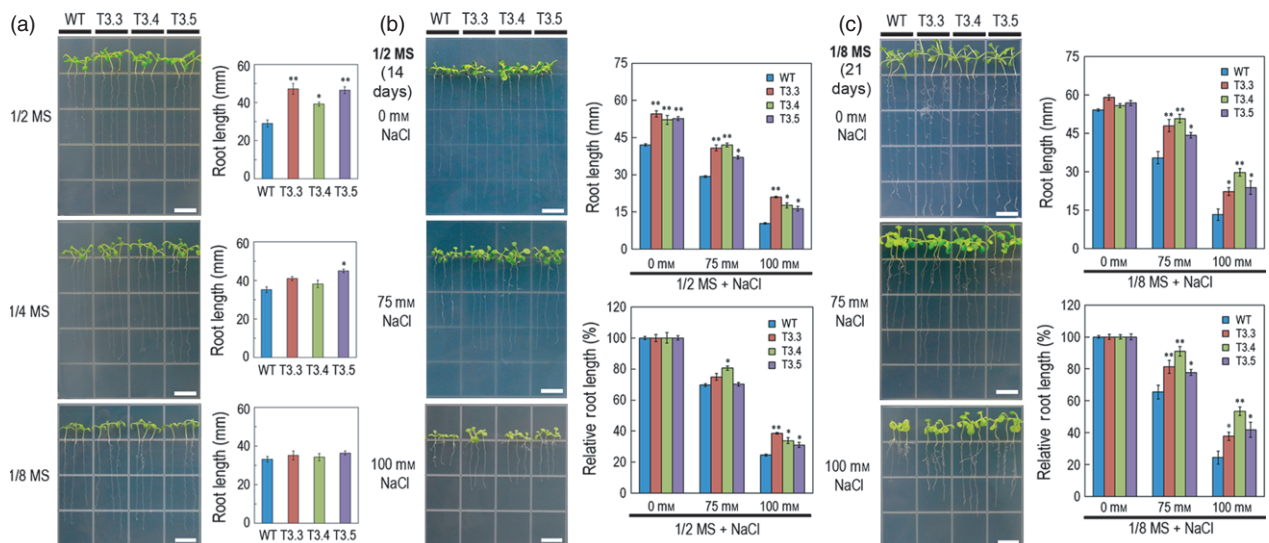


**Figure 5** Phenotypes of wild-type (WT) and *PutVHA-c* transgenic *Arabidopsis* grown under NaCl stress conditions. (a) Growth and root lengths of WT and transgenic seedlings (T3.3–T3.5) on vertical plates containing 1/2 MS, 1/4 MS and 1/8 MS medium; (b and c) growth, root lengths and relative root length of WT and transgenic seedlings (T3.3–T3.5) on vertical plates containing 1/2 (b) and 1/8 MS (c) media with 0, 75 and 100 mM NaCl. Plants were grown for the indicated number of days. Error bars represent SE ( $n = 9$ ). Asterisks indicate a significant difference between WT and transgenic plants ( $*P < 0.05$ ;  $**P < 0.01$ ). Scale bar = 1 cm.

*PutVHA-c* overexpression in *Arabidopsis* promotes plant growth and development by influencing V-ATPase-dependent endosomal trafficking.

## Discussion

### Influence of *PutVHA-c* on V-ATPase activity and plant growth

Plant V-ATPases are responsible for the acidification of organelles through proton transport (Kluge *et al.*, 2003). The VHA-c

of the  $V_0$  complex is essential for driving the proton transport (Forgac, 2007). An inhibitor of V-ATPase activity, ConcA, inhibited proton transport by specifically binding to the VHA-c. This finding shows that VHA-c is an essential subunit required for V-ATPase activity (Huss *et al.*, 2002). Characterization of plant mutants deficient in V-ATPase subunits has shown that V-ATPase activity is essential for plant growth. For example, the *atvha-c (det3)* mutant displayed approximately 40% of WT V-ATPase activity, a dramatic reduction in root growth and severe dwarfism (Ferjani *et al.*, 2013; Schumacher *et al.*, 1999). More-

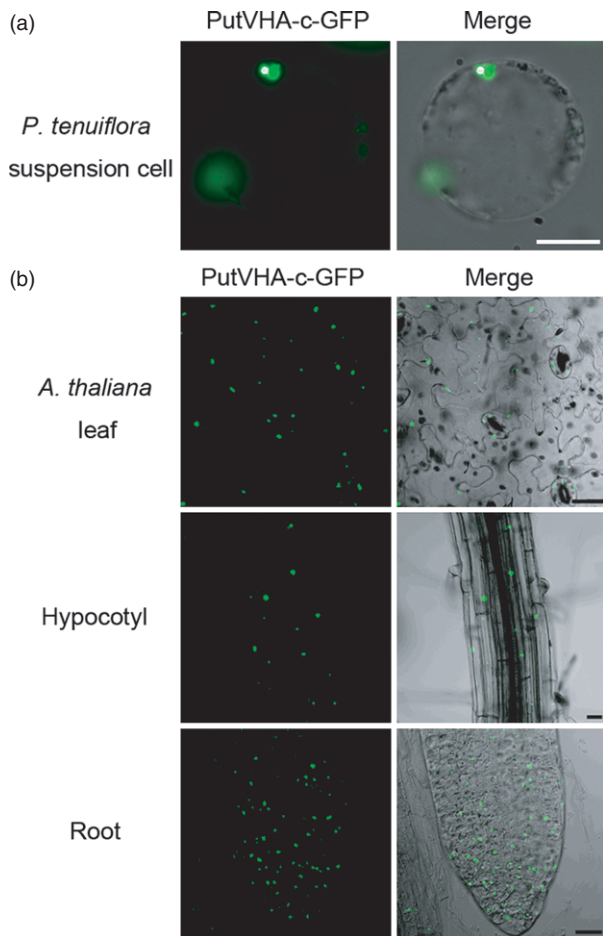


**Figure 6** Fluorescence patterns of PutVHA-c-GFP in *P. tenuiflora* suspension cells and *Arabidopsis*. (a) Fluorescence pattern of PutVHA-c-GFP in *P. tenuiflora* suspension cells; (b) fluorescence pattern of PutVHA-c-GFP in the leaf, hypocotyl and root epidermal cells of transgenic *Arabidopsis* seedlings. DIC: differential interference contrast. Scale bars = 20  $\mu\text{m}$ .

over, RNAi-mediated inhibition of *AtVHA-c1* or *AtVHA-c3* in *Arabidopsis* also reduced V-ATPase activity and root growth (Padmanaban *et al.*, 2004). Similarly, in this study, we found that the *atvha-c5* mutant showed reduced V-ATPase activity (Figure 4c) and retarded root growth (Figure 4d–f), while *PutVHA-c* overexpression in *Arabidopsis* enhanced V-ATPase activity (Table 1) and promoted plant growth (Figure 3). We also demonstrated that inhibition of V-ATPase activity by ConCA inhibited root growth of both WT and *PutVHA-c* transgenic seedlings (Figure S5). Our results agree with studies using other VHA subunits and further confirm that V-ATPase is important to plant growth and development.

#### Potential role of PutVHA-c in endosomal trafficking

It remains to be elucidated how the V-ATPase influences plant growth. In our study, PutVHA-c-GFP was detected in the punctate structures of protoplasts of *P. tenuiflora* (Figure 6a) and *Arabidopsis* (Figure 7b). PutVHA-c-GFP was colocalized with the FM4-64-labelled endosomes in root cells (Figure 7c–f). Immunogold electron microscopy observations also showed that PutVHA-c-GFP was localized in endosomes with various sizes (Figure 8). The size of the endosomes outlined by FM4-64 and gold particles was

estimated to be 0.1–1  $\mu\text{m}$ . We therefore suggest that the majority of these endosomes may be the prevacuolar compartment (PVC) or multivesicular body (MVB) or late endosomes (LE) (Figure 10a) as shown before for other VHA subunits (Herman *et al.*, 1994). These results suggest that PutVHA-c is mainly localized to the PVC/MVB/LE. However, we cannot entirely exclude the possibility that some small endosomes (such as Figure 7c and 8c) are the *trans*-Golgi network (TGN) or early endosomes (EE). Moreover, previous reports have also shown that the PVC/MVB/LE is derived from the TGN/EE through maturation (Scheuring *et al.*, 2011). Previous studies have shown that the V-ATPase inhibitor ConCA induces the aggregation of large Golgi-derived endosomes in the WT root cells (Figure 9b). ConCA treatment also induced aggregation of the PutVHA-c-GFP-labelled endosomes in *PutVHA-c-GFP* transgenic *Arabidopsis* (Figure 9d). These results indicate that the reduction of V-ATPase activity by ConCA blocks endosomal trafficking (Figure 10b).

In plant cells, endosomes serve as cargo carriers. Extracellular proteins, PM proteins and components of the cell wall, which regulate plant growth and environmental stimuli responses, are transported to the sites where they function via endosome-mediated trafficking (Battey and Blackbourn, 1993; Contento and Bassham, 2012; Cosgrove, 2005; Jürgens and Geldner, 2002). Previous study has shown that ConCA blocks the trafficking of newly synthesized PM proteins to the PM (Cai *et al.*, 2011; Dettmer *et al.*, 2006; Viotti *et al.*, 2010). Reduced endosomal V-ATPase activity might indirectly affect secretory trafficking of cell wall components (Brüx *et al.*, 2008). In our study, ConCA blocks the trafficking of PM proteins AtPIN1 and AtRGS1 to the PM (Figure 9f,h). Similarly,  $\text{H}^+$ -Pyrophosphatases (V-PPase or AVP) affects PIN1 trafficking likely by endosomal trafficking (Li *et al.*, 2005). The V-PPase and V-ATPase are endomembrane proton pumps, and their function is similar (Gaxiola *et al.*, 2007; Schumacher, 2006). Therefore, the endosome-mediated transport of functional PM proteins or cargoes should contribute to plant growth, development and environmental stress responses (Robinson *et al.*, 2012).

Further, our results showed that *PutVHA-c* overexpression enhanced  $\text{Na}^+$  efflux in the roots of transgenic *Arabidopsis* (Figure S6) and alleviated the inhibition of NaCl stress on the root growth (Figure 5b,c). ConCA treatment experiment showed that reduction of V-ATPase activity blocks PM proteins (AtPIN1 and AtRGS1) sorting (Figure 9e–h). Therefore, we speculate that an increase in V-ATPase activity due to *PutVHA-c* overexpression result in acceleration of PM proteins sorting, some of which respond to NaCl stress. One example is salt overly sensitive 1 (SOS1), a PM  $\text{Na}^+/\text{H}^+$ -antiporter that reduces the toxicity of  $\text{Na}^+$  by being involved in the exclusion of intercellular  $\text{Na}^+$  from cells (Oh *et al.*, 2010; Zhu, 2003). However, this hypothesis needs more evidence. On the basis of these information, we hypothesized that overexpression of *PutVHA-c* maybe accelerates the endosomal trafficking by enhancing V-ATPase activity and thereby promotes plant growth (Figure 10c).

## Experimental procedures

### Identification of *PutVHA-c* gene and sequence analysis

The sequencing of 3000 clones from a cDNA library of *Puccinellia tenuiflora* identified a cDNA clone with high sequence similarity to the sequences of known plant VHA-c genes. This clone was

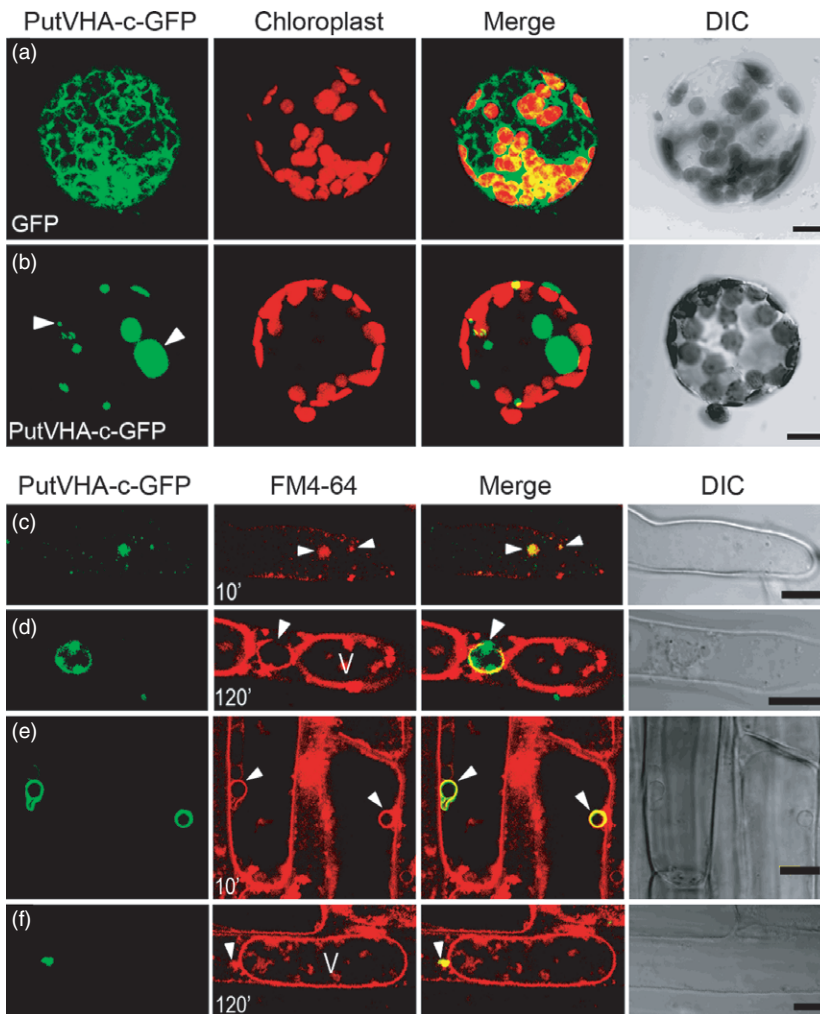


**Figure 7** Subcellular localization of PutVHA-c-GFP in transgenic *Arabidopsis*. (a and b) Confocal images of *Arabidopsis* mesophyll protoplasts with the stable expression of GFP alone (a) or PutVHA-c-GFP (b). Arrowheads indicate the punctate structures of different size. Solid punctate GFP signals are actually hollow structures in the microscope (b). Chlorophyll autofluorescence is shown in red; (c–f) seedlings root hair (c, d) and epidermal (e, f) cells expressing PutVHA-c-GFP (green) were incubated for 10 or 120 min with 4  $\mu\text{M}$  FM4-64 (red). Arrowhead indicates colocalization of PutVHA-c-GFP and FM4-64 in endosomal compartment. V: vacuole. Scale bars = 10  $\mu\text{m}$ .

named *PutVHA-c* (GenBank accession number: KJ184573) on the basis of its sequence similarity to the well-known *VHA-c* genes. Amino acid sequences of PutVHA-c and its homologs were aligned using Clustal W. The transmembrane domains in PutVHA-c were predicted by the TMHMM algorithm (<http://www.cbs.dtu.dk/services/TMHMM>).

#### Plant materials and growth conditions

*P. tenuiflora* seedlings were grown in pots containing a mixture of turf peat and sand (2:1 v/v). Plants were grown under controlled greenhouse conditions of 70%–80% relative humidity, 14 h of light and an average temperature of 22 °C. For salt and alkali treatment, 2-week-old hydroponically grown *P. tenuiflora* seedlings were treated with 200 mM NaCl, 20 mM Na<sub>2</sub>CO<sub>3</sub> or 100 mM NaHCO<sub>3</sub>. The leaves and roots from at least 20 seedlings from each treatment were harvested and pooled following different treatment time points (0, 6, 12 or 24 h), frozen immediately in liquid nitrogen and stored at –80 °C for RNA preparation.

All *Arabidopsis thaliana* plants used in this study belonged to the Columbia-0 (Col-0) ecotype. The seeds were surface sterilized and stratified at 4 °C for 2 days in the dark. The seedlings were then grown on 1/2 × Murashige and Skoog (MS) medium (Murashige and Skoog, 1962) (3% sucrose, 1% agar, pH 5.8), 1/4 × MS medium or 1/8 × MS medium under a 12/12-h light/dark photoperiod (100  $\mu\text{mol m}^{-2} \text{s}^{-1}$  light intensity) at 22 °C, unless otherwise stated.

#### Vector construction and *Arabidopsis* transformation

The ORF of *PutVHA-c* was amplified from *PutVHA-c* cDNA using the primers pBI121-F (5'-GGATCCATGTCGCGGTGTTTC-3') and pBI121-R (5'-GTCGACCTAATCTGCGCGGGAT-3'). The *Bam*HI and *Sal*I sites are underlined. The amplified fragments were cloned into the pBI121 vector to generate the plasmid pBI121-PutVHA-c. To construct the *GFP* fusion genes, the ORF of *PutVHA-c* without the stop codon was amplified using the primers pBI121-F and GFP-R (5'-GGTACCAAATCTGCGCGGG-3'; the *Kpn*I site is underlined) and then cloned into the pEGFP vector. The *PutVHA-c-GFP* fusion gene was amplified with the primers pBI121-F and 121-GFP-R (5'-GTCGACTTACTTGTA-CAGCTCGTC-3'; the *Sal*I site is underlined) and then cloned into the *Bam*HI and *Sal*I sites of pBI121 vector. The ORF of *AtVHA-c3* was amplified from *AtVHA-c3* cDNA using the primers pBI121-F1 (5'-GGATCCATGTCCTACCTTCAGTG-3') and pBI121-R1 (5'-GTC-GACTCATTGCGCTCTGGACTG-3'). The *Bam*HI and *Sal*I sites are underlined. The amplified fragments were cloned into the pBI121 vector to generate the plasmid pBI121-AtVHA-c3. To construct the *GFP* fusion genes, the ORF of *AtVHA-c3* without the stop codon was amplified using the primers pBI121-F1 and GFP-R1 (5'-GGTACCTTTTCGGCTCTGGAC-3'; the *Kpn*I site is underlined) and then cloned into the pEGFP vector. The *AtVHA-c3-GFP* fusion gene was amplified with the primers pBI121-F1 and 121-GFP-R (5'-GTCGACTTACTTGTA-CAGCTCGTC-3'; the *Sal*I site is under-

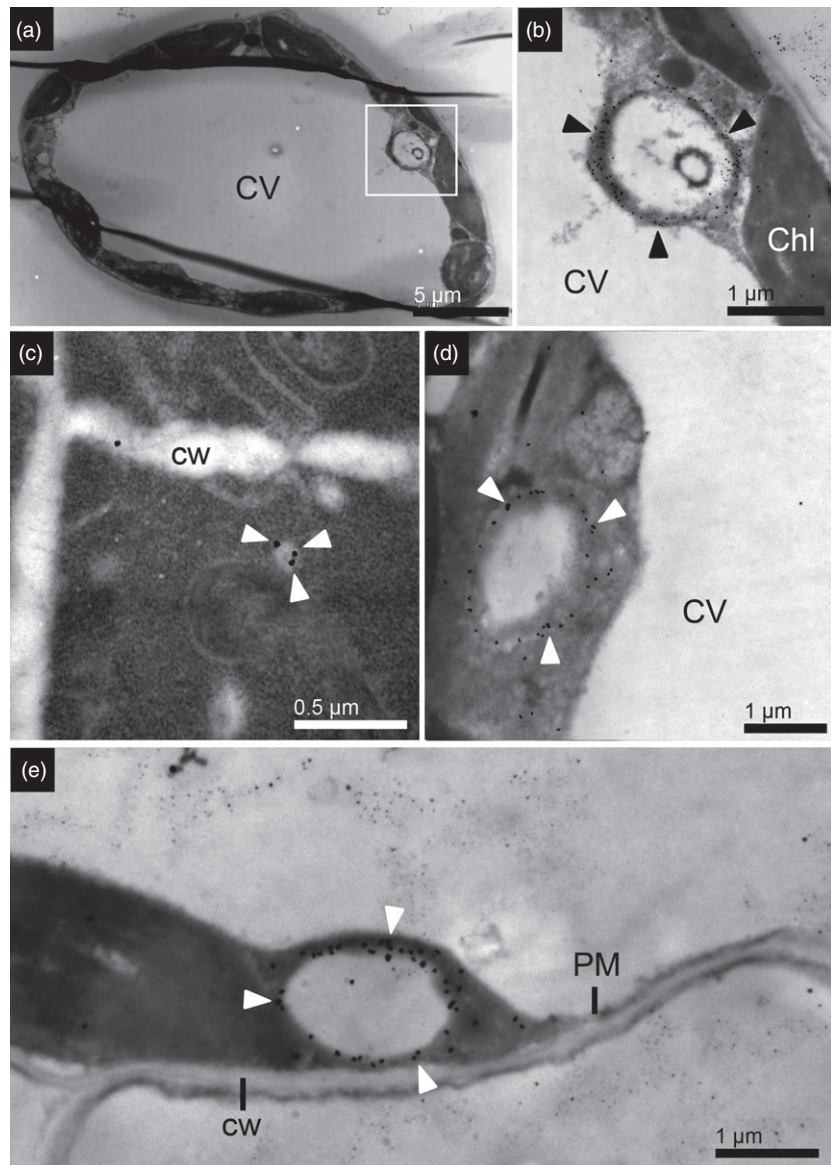


**Figure 8** Immunogold localization of PutVHA-c-GFP in transgenic *Arabidopsis*. The PutVHA-c-GFP in ultrathin leaf sections reacted with an anti-GFP antibody and a gold-conjugated secondary antibody. The gold particles were detected by transmission electron microscopy. (a) Immunogold labelling of PutVHA-c-GFP in a leaf from a transgenic *Arabidopsis* plant; (b) higher magnification of the boxed area in the panel (a). Gold particles (arrowhead) accumulated primarily in the endosomal membrane; (c–e) gold particles (arrowhead) specifically accumulated in the endosomes of various sizes. These endosomes were distributed in the cytoplasm (c) and close to the central vacuole (d) or PM (e). Chl, chloroplast; CV, central vacuole; PM, plasma membrane; cw, cell wall. Scale bars = 5 µm (a), 0.5 µm (c) and 1 µm (b, d, e).

lined) and then cloned into the *Bam*HI and *Sal*I sites of pBI121 vector. The plasmids, pBI121-PutVHA-c, pBI121-PutVHA-c-GFP, pBI121-AtVHA-c3 and pBI121-AtVHA-c3-GFP were sequenced and transformed into *Agrobacterium tumefaciens* strain EHA105 for plant transformation. *Arabidopsis* was transformed using the floral dip method (Clough and Bent, 1998). Transgenic plants were selected using  $1/2\times$  MS media containing  $30\ \mu\text{g mL}^{-1}$  kanamycin. Expression of the *PutVHA-c* in transgenic lines was assessed by northern blot analyses. The T3 generation was used for the analyses.

#### Identification of mutants

The *AtVHA-c5* T-DNA insertion mutant SAIL\_654\_E11 (CS828396) was obtained from the Arabidopsis Biological Resource Center (ABRC: <http://www.arabidopsis.org/>). Molecular characterization of the mutant was performed using genomic DNA isolated from 4-week-old WT (Col-0) and *atvha-c5* leaves using the primers AT2G16510\_LP (5'-TATTTGACGGATACGCTCA CC-3'), AT2G16510\_RP (5'-CTTCTGTTGTTTCAGGCAAGC-3')

and LB-3 (5'-TAGCATCTGAATTCATAACCAATCTCGATACAC-3'). Expression of the *AtVHA-c5* in mutant SAIL\_654\_E11 was assessed by real-time quantitative PCR analyses.

#### Characterization of plant growth phenotypes

Soil-grown *Arabidopsis* plants were maintained in greenhouse conditions (22 °C day/night temperature, 16/8-h light/dark regime of approximately  $100\ \mu\text{mol m}^{-2}\ \text{s}^{-1}$  illumination and 60%–80% relative humidity). For mature plant phenotypes, WT and transgenic *Arabidopsis* plants were grown side by side in a growth chamber. After examining growth phenotypes, the plants were photographed. Images were processed using Adobe Photoshop CS.

For NaCl stress tests, the *Arabidopsis* seeds were treated at 4 °C for 2 days and then grown for 14 days before measurements were taken of root lengths on  $1/2\times$  MS media containing 0, 75 or 100 mM NaCl. Additionally, the seeds were germinated on  $1/8\times$  MS medium and grown for 5 days. The seedlings were subsequently transferred to  $1/8\times$  MS media containing 0, 75 or 100 mM NaCl for 16 days.

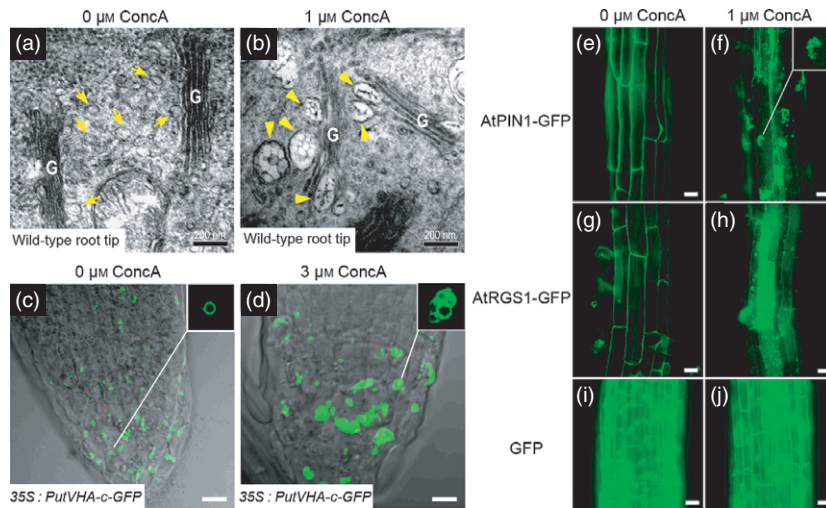


**Figure 9** ConcA treatment induced the aggregation of endosomal compartments and blocked the trafficking of plasma membrane proteins AtPIN1-GFP and AtRGS1-GFP. Wild-type (WT) and transgenic *Arabidopsis* seedlings (4-day-old) expressing PutVHA-c-GFP, AtPIN1-GFP, AtRGS1-GFP or GFP alone were incubated for 3 h in liquid 1/2 MS medium and the indicated concentrations of ConcA and were then used for transmission electron microscope (TEM) or confocal laser scanning microscopy (CLSM). (a and b) Electron micrographs of root tip cortex cells from WT *Arabidopsis*. Arrows indicate the morphology of the Golgi-derived endosomes in untreated cells (a). Arrowheads indicate the aggregation of large Golgi-derived endosomes in ConcA-treated cells (b); (c) untreated seedling root cells expressing PutVHA-c-GFP; (d) ConcA-treated seedling root cells expressing PutVHA-c-GFP. Shown are overlays of the GFP and DIC channels (c and d). Insets in panels (c) and (d) show the close-up images of the PutVHA-c-GFP signals in the GFP channel; (e–j) untreated seedling root cells expressing AtPIN1-GFP (e), AtRGS1-GFP (g) or GFP alone (i); ConcA-treated seedling root cells expressing AtPIN1-GFP (f), AtRGS1-GFP (h) or GFP alone (j). Insets in panels (f) show the close-up images of the AtPIN1-GFP signals in the interior of the root cells. G, Golgi. Scale bars = 200 nm (a and b), 10  $\mu\text{m}$  (c and d) and 20  $\mu\text{m}$  (e–j).

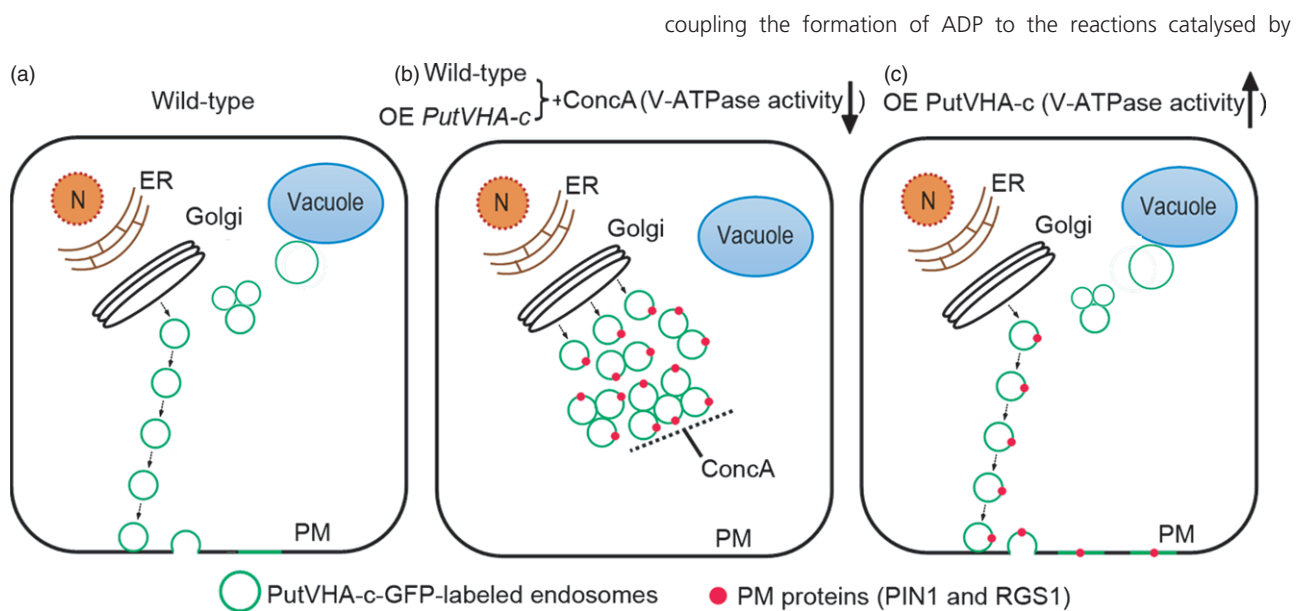


**Figure 10** Model of PutVHA-c involvement in endosomal trafficking. (a) Our results showed that PutVHA-c is mainly localized to the endosomal compartment; (b) reduction of V-ATPase activity by ConcA causes the aggregation of large Golgi-derived endosomes and blocks the trafficking of two PM proteins AtPIN1-GFP and AtRGS1-GFP to the PM; (c) overexpression of *PutVHA-c* may accelerate the endosomal trafficking by increasing the V-ATPase activity. OE, overexpression; N, nucleus; ER, endoplasmic reticulum; PM, plasma membrane.

### V-ATPase activity measurements

The extraction of microsomal proteins was performed according to a previously described procedure (Tang *et al.*, 2012). V-ATPase activity was measured using the V-type ATPase Activity Assay Kit (Genmed Scientifics Inc., Arlington, MA). This procedure involves

coupling the formation of ADP to the reactions catalysed by

pyruvate kinase and lactate dehydrogenase with NADH oxidation in the presence of both the F-type ATPase inhibitor oligomycin and the P-type ATPase inhibitor orthovanadate. The disappearance of NADH is detected by measuring a decrease in extinction at 340 nm (Palmgren, 1990). The experiment was repeated three times.

### Protein localization using confocal laser scanning microscopy

Four- to five-day-old seedlings grown on vertical 1/2× MS agar plates were incubated in 1 mL of liquid 1/2× MS media (0.5% sucrose, pH 5.8) that contained 4 μM FM4-64 (Invitrogen, Carlsbad, CA) for 2–120 min at room temperature. Seedlings were washed twice with the liquid 1/2× MS medium immediately before confocal laser scanning microscopy (CLSM) (Olympus Fluoview FV500, Tokyo, Japan). GFP signals were detected using a 500–530 nm emission filter. FM4-64 signals were detected using a 620–680 nm emission filter.

### Inhibitor (ConcA) treatments

For concanamycin A (ConcA) (Sigma-Aldrich, St. Louis, MO) treatment of seedlings grown on plates, the seeds were surface sterilized and stratified at 4 °C for 2 days in the dark. The seedlings were then grown on 1/2× MS media containing 0, 0.3 or 0.6 μM ConcA under a 12/12-h light/dark photoperiod (100 μmol m<sup>-2</sup> s<sup>-1</sup> light intensity) at 22 °C.

To examine the effect of ConcA on protein localization, the 4-day-old seedlings grown on vertical 1/2× MS agar medium were incubated in 1 mL of liquid 1/2× MS media (0.5% sucrose, pH 5.8), containing either 1 or 3 μM ConcA. The incubation lasted for 3 h at room temperature after which the seedlings were immediately used for the CLSM.

### Structure analysis, immunogold labelling and electron microscopy

To observe the ConcA-induced structures in *Arabidopsis* root cells, 4-day-old root tips from wild-type *Arabidopsis* were incubated in 1 mL of liquid 1/2× MS media (0.5% sucrose, pH 5.8) containing 1 μM ConcA. Again, incubation lasted for 3 h at room temperature. Roots were incubated in the fixation solution (2.5% [v/v] glutaraldehyde in 0.1 M phosphate buffer, pH 7.4) under a vacuum for 4 h. The root tips of the fixed plants were dehydrated in ethanol and embedded in LR White resin (Sigma-Aldrich). The resin was incubated at 50 °C for 12 h for polymerization. Ultrathin (60–80 nm) sections of the resin were prepared using a Leica EM UC6 ultramicrotome (Leica, Vienna, Austria) and were placed on formvar-coated nickel grids. The sections were poststained with uranyl acetate and lead citrate and were used for electron microscopy with a H-7500 transmission electron microscope (Hitachi, Tokyo, Japan), which was operated set at 80 kv.

Immunogold labelling was performed according to a previously described procedure (Zhang *et al.*, 2001), with the following modifications. Four-day-old seedlings grown on 1/2× MS agar plates were fixed and dehydrated in the reagents specified in the preceding paragraph. Tissues (root tips and leaves) were embedded in LR White resin (Sigma-Aldrich). Ultrathin sections of 80–100 nm were placed on formvar-coated nickel grids. The sections were allowed to react with a mouse anti-GFP antibody (Roche, Burgess Hill, West Sussex, UK) that was diluted 200 times in the reaction buffer (1× PBS containing 1% BSA and 0.2% Tween-20). Sections were incubated overnight at 4 °C and then allowed to react with a gold-conjugated (10 nm) rabbit anti-mouse IgG antibody (Sigma-Aldrich), which was diluted in the stated reaction buffer for 2 h at room temperature. Finally, the sections were incubated in silver lactate (Sigma-Aldrich) for 15 min at room temperature. The sections were poststained with aqueous uranyl acetate, and the gold particles were detected using a transmission electron microscope (Hitachi).

### Statistical analyses

The data were analysed using one-way analysis of variance by SPSS, and statistically significant differences were calculated based on Student's t-test, with  $P < 0.05$  (\*) and  $P < 0.01$  (\*\*) as thresholds for significance.

### Acknowledgements

This work was supported by Program for Changjiang Scholars and Innovative Research Team in University of China (IRT13053). We thank Prof. Jirong Huang (Chinese Academy of Sciences, China) for providing the *GmMan1-YFP*, *AtγTIP-GFP* and *AtRGS1-GFP* transgenic *Arabidopsis* seeds, and Prof. Yuxiang Cheng (Northeast Forestry University, China) for providing the *pin1pro::AtPIN1-GFP* transgenic *Arabidopsis* seeds. We thank Prof. Jirong Huang (Chinese Academy of Sciences, China), Dr. Xiaoli Sun, Prof. Yanming Zhu (Northeast Agricultural University, China) and Dr. Daisuke Tsugama (University of Tokyo, Japan) for constructive comments on the manuscript. We also thank the staff at Editage for copy editing the manuscript.

### References

- Baisakh, N., RamanaRao, M.V., Rajasekaran, K., Subudhi, P., Janda, J., Galbraith, D., Vanier, C. and Pereira, A. (2012) Enhanced salt stress tolerance of rice plants expressing a vacuolar H<sup>+</sup>-ATPase subunit c1 (*SaVHAc1*) gene from the halophyte grass *Spartina alterniflora* Loisel. *Plant Biotechnol. J.* **10**, 453–464.
- Bassham, D.C., Brandizzi, F., Otegui, M.S. and Sanderfoot, A.A. (2008) The secretory system of *Arabidopsis*. *Arabidopsis Book*, **6**, e0116.
- Batley, N.H. and Blackbourn, H.D. (1993) The control of exocytosis in plant cells. *New Phytol.* **125**, 307–331.
- Bolte, S., Talbot, C., Boutte, Y., Catrice, O., Read, N.D. and Satiat-Jeunemaitre, B. (2004) FM- dyes as experimental probes for dissecting vesicle trafficking in living plant cells. *J. Microsc.* **214**, 159–173.
- Bowman, E.J., Graham, L.A., Stevens, T.H. and Bowman, B.J. (2004) The bafilomycin/concanamycin binding site in subunit c of the V-ATPases from *Neurospora crassa* and *Saccharomyces cerevisiae*. *J. Biol. Chem.* **279**, 33131–33138.
- Brüx, A., Liu, T.Y., Krebs, M., Stierhof, Y.D., Lohmann, J.U., Miersch, O., Wasternack, C. and Schumacher, K. (2008) Reduced V-ATPase activity in the *trans*-Golgi network causes oxylipin-dependent hypocotyl growth inhibition in *Arabidopsis*. *Plant Cell*, **20**, 1088–1100.
- Cai, Y., Jia, T., Lam, S.K., Ding, Y., Gao, C., San, M.W., Pimpl, P. and Jiang, L. (2011) Multiple cytosolic and transmembrane determinants are required for the trafficking of SCAMP1 via an ER-Golgi-TGN-PM pathway. *Plant J.* **65**, 882–896.
- Chen, J.G., Willard, F.S., Huang, J.R., Liang, J., Chasse, S.A., Jones, A.M. and Siderovski, D.P. (2003) A seven-transmembrane RGS protein that modulates plant cell proliferation. *Science*, **301**, 1728–1731.
- Clough, S.J. and Bent, A.F. (1998) Floral dip: a simplified method for *Agrobacterium*-mediated transformation of *Arabidopsis thaliana*. *Plant J.* **16**, 735–743.
- Contento, A.L. and Bassham, D.C. (2012) Structure and function of endosomes in plant cells. *J. Cell Sci.* **125**, 3511–3518.
- Cosgrove, D.J. (2005) Growth of the plant cell wall. *Nat. Rev. Mol. Cell Biol.* **6**, 850–861.
- Dettmer, J., Hong-Hermesdorf, A., Stierhof, Y.D. and Schumacher, K. (2006) Vacuolar H<sup>+</sup>-ATPase activity is required for endocytic and secretory trafficking in *Arabidopsis*. *Plant Cell*, **18**, 715–730.
- Ferjani, A., Ishikawa, K., Asaoka, M., Ishida, M., Horiguchi, G., Maeshima, M. and Tsukaya, H. (2013) Enhanced cell expansion in a KRP2 overexpressor is mediated by increased V-ATPase activity. *Plant Cell Physiol.* **54**, 1989–1998.

- Forgac, M. (2007) Vacuolar ATPases: rotary proton pumps in physiology and pathophysiology. *Nat. Rev. Mol. Cell Biol.* **8**, 917–929.
- Gao, C., Wang, Y., Jiang, B., Liu, G., Yu, L., Wei, Z. and Yang, C. (2011) A novel vacuolar membrane H<sup>+</sup>-ATPase c subunit gene (*ThVHAc1*) from *Tamarix hispida* confers tolerance to several abiotic stresses in *Saccharomyces cerevisiae*. *Mol. Biol. Rep.* **38**, 957–963.
- Gaxiola, R.A., Palmgren, M.G. and Schumacher, K. (2007) Plant proton pumps. *FEBS Lett.* **581**, 2204–2214.
- Geldner, N., Friml, J., Stierhof, Y.D., Jurgens, G. and Palme, K. (2001) Auxin transport inhibitors block PIN1 cycling and vesicle trafficking. *Nature*, **413**, 425–428.
- Herman, E.M., Li, X., Su, R.T., Larsen, P., Hsu, H. and Sze, H. (1994) Vacuolar-type H<sup>+</sup>-ATPases are associated with the endoplasmic reticulum and provacuoles of root tip cells. *Plant Physiol.* **106**, 1313–1324.
- Hirata, T., Iwamoto-Kihara, A., Sun-Wada, G.H., Okajima, T., Wada, Y. and Futai, M. (2003) Subunit rotation of vacuolar-type proton pumping ATPase: relative rotation of the G and C subunits. *J. Biol. Chem.* **278**, 23714–23719.
- Hu, G.Z., Suo, Y.P. and Huang, J.R. (2013) A crucial role of the RGS domain in *trans*-Golgi network export of AtRGS1 in the protein secretory pathway. *Mol. Plant*, **6**, 1933–1944.
- Huss, M., Ingenhorst, G., Konig, S., Gassel, M., Drose, S., Zeeck, A., Altendorf, K. and Wieczorek, H. (2002) Concanamycin A, the specific inhibitor of V-ATPases, binds to the V(0) subunit c. *J. Biol. Chem.* **277**, 40544–40548.
- Jürgens, G. and Geldner, N. (2002) Protein Secretion in Plants: from the *trans*-Golgi network to the outer space. *Traffic*, **3**, 605–613.
- Kluge, C., Lahr, J., Hanitzsch, M., Bolte, S., Gollmack, D. and Dietz, K.J. (2003) New insight into the structure and regulation of the plant vacuolar H<sup>+</sup>-ATPase. *J. Bioenerg. Biomembr.* **35**, 377–388.
- Krebs, M., Beyhl, D., Gorlich, E., Al-Rasheid, K.A., Marten, I., Stierhof, Y.D., Hedrich, R. and Schumacher, K. (2010) Arabidopsis V-ATPase activity at the tonoplast is required for efficient nutrient storage but not for sodium accumulation. *Proc. Natl Acad. Sci. USA*, **107**, 3251–3256.
- Kreck, P., Skupa, P., Libus, J., Naramoto, S., Tejos, R., Friml, J. and Zazimalova, E. (2009) The PIN-FORMED (PIN) protein family of auxin transporters. *Genome Biol.* **10**, 249.
- Li, J., Yang, H., Peer, W.A., Richter, G., Blakeslee, J., Bandyopadhyay, A., Titapiwantakun, B., Undurraga, S., Khodakovskaya, M., Richards, E.L., Krizek, B., Murphy, A.S., Gilroy, S. and Gaxiola, R. (2005) Arabidopsis H<sup>+</sup>-PPase AVP1 regulates auxin-mediated organ development. *Science*, **310**, 121–125.
- Löw, R., Rockel, B., Kirsch, M., Ratajczak, R., Hortensteiner, S., Martinoia, E., Lutge, U. and Rausch, T. (1996) Early salt stress effects on the differential expression of vacuolar H(+)ATPase genes in roots and leaves of *Mesembryanthemum crystallinum*. *Plant Physiol.* **110**, 259–265.
- Marshansky, V. and Futai, M. (2008) The V-type H<sup>+</sup>-ATPase in vesicular trafficking: targeting, regulation and function. *Curr. Opin. Cell Biol.* **20**, 415–426.
- Matsuoka, K., Higuchi, T., Maeshima, M. and Nakamura, K. (1997) A vacuolar-type H<sup>+</sup>-ATPase in a nonvacuolar organelle is required for the sorting of soluble vacuolar protein precursors in tobacco Cells. *Plant Cell*, **9**, 533–546.
- Murashige, T. and Skoog, F. (1962) A revised medium for rapid growth and bioassays with tobacco tissue cultures. *Physiol. Plant.* **15**, 473–495.
- Nishi, T. and Forgac, M. (2002) The vacuolar (H<sup>+</sup>)-ATPases—nature's most versatile proton pumps. *Nat. Rev. Mol. Cell Biol.* **3**, 94–103.
- Noumi, T., Beltran, C., Nelson, H. and Nelson, N. (1991) Mutational analysis of yeast vacuolar H(+)ATPase. *Proc. Natl Acad. Sci. USA*, **88**, 1938–1942.
- Oh, D.H., Lee, S.Y., Bressan, R.A., Yun, D.J. and Bohnert, H.J. (2010) Intracellular consequences of SOS1 deficiency during salt stress. *J. Exp. Bot.* **61**, 1205–1213.
- Padmanaban, S., Lin, X., Perera, I., Kawamura, Y. and Sze, H. (2004) Differential expression of vacuolar H<sup>+</sup>-ATPase subunit c genes in tissues active in membrane trafficking and their roles in plant growth as revealed by RNAi. *Plant Physiol.* **134**, 1514–1526.
- Palmgren, M.G. (1990) An H<sup>+</sup>-ATPase assay: proton pumping and ATPase activity determined simultaneously in the same sample. *Plant Physiol.* **94**, 882–886.
- Perera, I.Y., Li, X. and Sze, H. (1995) Several distinct genes encode nearly identical to 16 kDa proteolipids of the vacuolar H(+)ATPase from *Arabidopsis thaliana*. *Plant Mol. Biol.* **29**, 227–244.
- Reichardt, I., Stierhof, Y.D., Mayer, U., Richter, S., Schwarz, H., Schumacher, K. and Jurgens, G. (2007) Plant cytokinesis requires de novo secretory trafficking but not endocytosis. *Curr. Biol.* **17**, 2047–2053.
- Richter, S., Voss, U. and Jurgens, G. (2009) Post-Golgi traffic in plants. *Traffic*, **10**, 819–828.
- Robinson, D.G., Albrecht, S. and Moriysu, Y. (2004) The V-ATPase inhibitors concanamycin A and bafilomycin A lead to Golgi swelling in tobacco BY-2 cells. *Protoplasma*, **224**, 255–260.
- Robinson, D.G., Jiang, L. and Schumacher, K. (2008) The endosomal system of plants: charting new and familiar territories. *Plant Physiol.* **147**, 1482–1492.
- Robinson, D.G., Pimpl, P., Scheuring, D., Stierhof, Y.D., Sturm, S. and Viotti, C. (2012) Trying to make sense of retromer. *Trends Plant Sci.* **17**, 431–439.
- Scheuring, D., Viotti, C., Kruger, F., Kunz, F., Sturm, S., Bubeck, J., Hillmer, S., Frigerio, L., Robinson, D.G., Pimpl, P. and Schumacher, K. (2011) Multivesicular bodies mature from the *trans*-Golgi network/early endosome in Arabidopsis. *Plant Cell*, **23**, 3463–3481.
- Schumacher, K. (2006) Endomembrane proton pumps: connecting membrane and vesicle transport. *Curr. Opin. Plant Biol.* **9**, 595–600.
- Schumacher, K. and Krebs, M. (2010) The V-ATPase: small cargo, large effects. *Curr. Opin. Plant Biol.* **13**, 724–730.
- Schumacher, K., Vafeados, D., McCarthy, M., Sze, H., Wilkins, T. and Chory, J. (1999) The Arabidopsis *det3* mutant reveals a central role for the vacuolar H (+)-ATPase in plant growth and development. *Genes Dev.* **13**, 3259–3270.
- Seidel, T., Kluge, C., Hanitzsch, M., Ross, J., Sauer, M., Dietz, K.J. and Gollmack, D. (2004) Colocalization and FRET-analysis of subunits c and a of the vacuolar H<sup>+</sup>-ATPase in living plant cells. *J. Biotechnol.* **112**, 165–175.
- Sun, Y., Li, H. and Huang, J.R. (2012) Arabidopsis TT19 functions as a carrier to transport anthocyanin from the cytosol to tonoplasts. *Mol. Plant*, **5**, 387–400.
- Sze, H., Schumacher, K., Muller, M.L., Padmanaban, S. and Taiz, L. (2002) A simple nomenclature for a complex proton pump: VHA genes encode the vacuolar H(+)ATPase. *Trends Plant Sci.* **7**, 157–161.
- Tang, R.J., Liu, H., Yang, Y., Yang, L., Gao, X.S., Garcia, V.J., Luan, S. and Zhang, H.X. (2012) Tonoplast calcium sensors CBL2 and CBL3 control plant growth and ion homeostasis through regulating V-ATPase activity in Arabidopsis. *Cell Res.* **22**, 1650–1665.
- Tsiantis, M.S., Bartholomew, D.M. and Smith, J.A. (1996) Salt regulation of transcript levels for the c subunit of a leaf vacuolar H(+)ATPase in the halophyte *Mesembryanthemum crystallinum*. *Plant J.* **9**, 729–736.
- Tyagi, W., Rajagopal, D., Singla-Pareek, S.L., Reddy, M.K. and Sopory, S.K. (2005) Cloning and regulation of a stress-regulated *Pennisetum glaucum* vacuolar ATPase c gene and characterization of its promoter that is expressed in shoot hairs and floral organs. *Plant Cell Physiol.* **46**, 1411–1422.
- Ueda, T., Yamaguchi, M., Uchimiya, H. and Nakano, A. (2001) Ara6, a plant-unique novel type Rab GTPase, functions in the endocytic pathway of *Arabidopsis thaliana*. *EMBO J.* **20**, 4730–4741.
- Umamoto, N., Yoshihisa, T., Hirata, R. and Anraku, Y. (1990) Roles of the VMA3 gene product, subunit c of the vacuolar membrane H(+)ATPase on vacuolar acidification and protein transport. A study with VMA3-disrupted mutants of *Saccharomyces cerevisiae*. *J. Biol. Chem.* **265**, 18447–18453.
- Urano, D., Phan, N., Jones, J.C., Yang, J., Huang, J., Grigston, J., Taylor, J.P. and Jones, A.M. (2012) Endocytosis of the seven-transmembrane RGS1 protein activates G-protein-coupled signalling in Arabidopsis. *Nat. Cell Biol.* **14**, 1079–1088.
- Viotti, C., Bubeck, J., Stierhof, Y.D., Krebs, M., Langhans, M., van den Berg, W., van Dongen, W., Richter, S., Geldner, N., Takano, J., Jurgens, G., de Vries, S.C., Robinson, D.G. and Schumacher, K. (2010) Endocytic and secretory traffic in Arabidopsis merge in the *trans*-Golgi network/early endosome, an independent and highly dynamic organelle. *Plant Cell*, **22**, 1344–1357.
- Zhang, D.P., Lu, Y.M., Wang, Y.Z., Duan, C.Q. and Yan, H.Y. (2001) Acid invertase is predominantly localized to cell walls of both the practically symplasmically isolated sieve element/companion cell complex and parenchyma cells in developing apple fruits. *Plant, Cell Environ.* **24**, 691–702.
- Zhu, J.K. (2003) Regulation of ion homeostasis under salt stress. *Curr. Opin. Plant Biol.* **6**, 441–445.

## Supporting information

Additional Supporting information may be found in the online version of this article:

**Figure S1** Sequence alignment of the VHA-c sequences from various plants.

**Figure S2** Alignment of amino acid sequences for PutVHA-c, and three AtVHA-c proteins from *Arabidopsis*.

**Figure S3** Seed size comparison of wild-type (WT) and transgenic *Arabidopsis*.

**Figure S4** Phenotypes of wild-type (WT) and transgenic *Arabidopsis* plants overexpressing AtVHA-c3.

**Figure S5** Concanamycin A (ConcA) affects the root growth of wild-type (WT) and PutVHA-c transgenic *Arabidopsis* seedlings.

**Figure S6** Net fluxes of Na<sup>+</sup> in the roots of wild-type (WT) and transgenic *Arabidopsis* plants overexpressing PutVHA-c.

**Figure S7** Comparison of fluorescence patterns of PutVHA-c-GFP and different organelles markers.

**Figure S8** Confocal images of *Arabidopsis* mesophyll protoplasts with the stable expression of AtVHA-c3-GFP.

**Figure S9** Time-course of the endosome marker FM4-64 in root cells of *Arabidopsis*.

**Figure S10** FM4-64 dye is transported to the vacuole membrane via endosomes.

**Figure S11** Localization of PutVHA-c-GFP in *Arabidopsis*.

**Data S1** Materials and methods.

## Data S1 Materials and methods

### Supplementary experimental procedures

#### Semi-quantitative PCR and northern blot analyses

Total RNA was extracted from *P. tenuiflora* using the RNeasy Mini Kit (Qiagen, Germany) according to the manufacturer's instructions. First-strand cDNA was synthesized from 1 µg of total RNA by using the M-MLV RTase cDNA Synthesis Kit (TaKaRa, Japan), and was then used to amplify *PutActin* or *PutVHA-c* cDNAs by PCR. Semi-quantitative PCR was performed by heating samples to 95°C for 5 min, followed by 25 or 28 cycles that each comprised incubation at 95°C (30 s), 60°C (30 s), and 72°C (60 s). The forward and reverse *PutVHA-c* primers recognized sequences that included the start and stop codons of the *PutVHA-c* ORF (*PutVHA-c*-F: 5'-ATGTCGTCGGTGTTCAGCGGAG-3'; *PutVHA-c*-R: 5'-CTAATCTGCGCGGGATTGGC-3'). The *PutActin* primers (*PutActin*-F: 5'-CACCATCACCAGAATCCAGC-3'; *PutActin*-R: 5'-TGAAGGATGGCTGGAAGAGG-3') amplified part of the coding region of the *PutActin* ORF.

Total RNA (7.5 µg) from *P. tenuiflora* was fractionated on 1% (m/v) agarose-formaldehyde gels and transferred onto Hybond N<sup>+</sup> membranes (Amersham Pharmacia Biotech, UK). Hybridization was performed at 50°C using a digoxigenin-labeled probe that targeted the coding region of *PutVHA-c*. Hybridization signals were detected with CDP-Star (Tropix, USA) using a LAS-1000plus image analyzer (FujiFilm, Japan).

#### Real-time quantitative PCR analyses

Total RNA was extracted from *Arabidopsis* using the RNeasy Mini Kit (Qiagen), according to the manufacturer's instructions. First-strand cDNA was synthesized from 1 µg of total RNA with the M-MLV RTase cDNA Synthesis Kit (TaKaRa, Shiga, Japan). Real-time quantitative PCR analysis was performed using the SYBR Green Mix (Agilent Technologies, Palo Alto, CA, USA) in an optical 96-well plate with the Mx3000P system (Agilent). The forward and reverse *AtVHA-c1~c5* (At4G34720, AT1G19910, AT4G38920, AT1G75630, AT2G16510) primers were c1-F (5'-CCTGTTGTTATGGCTGGAGTG-3'), c1-R (5'-GTGCGTATCCATCAAAGAGGTAG-3'); c2-F (5'-GCTGAAGCACTTGCCCTGTA-3'), c2-R (5'-CTCTGGATTTCACTCGGCTC-3'); c3-F (5'-TTCGCTGAAGCTCTTGCTCT-3'), c3-R (5'-TTCTCATTCGGCTCTGGACT-3'); c4-F

(5'-GGAGCAACAGTCATCAAAGAGC-3'), c4-R (5'-A CTCCACTCTTCGCCGTC-3'); c5-F (5'-ACGGATACGCTCACCTTTCG-3') and c5-R (5'-ACACCCGCATCACCAACAAT-3'). *AtActin2* (AT3G18780) was selected as a reference gene, and the primer sequences used to quantify the abundance of *AtActin2* transcripts were 5'-GGTAACA TTGTGCTCAGTGGTGG-3' and 5'-AACGACCTTAATCTTCATGCTGC-3'.

#### **Promoter-GUS fusion analysis and histochemical assay of GUS activity**

To construct *AtVHA-c1~c3:GUS*, we amplified promoter regions of three *AtVHA-c* genes from Col-0 genomic DNA. The promoter regions were 0.5 kb, 2.2 kb, and 1.0 kb for *AtVHA-c1*, *AtVHA-c2*, *AtVHA-c3* genes, respectively, and were located immediately upstream of the ATG start codon. The regions were verified with sequencing. The PCR fragment was cloned into the *Hind* III/*Xba* I site of binary vector pBI121 to obtain a transcriptional fusion of the *AtVHA-c1~c3* promoter with the GUS coding sequence. To generate the *AtVHA-c4:GUS* construct, 1.6 kb of the *AtVHA-c4* promoter region was amplified using Col-0 genomic DNA and cloned into the *Hind*III/*Sma*I site of pBI121 vector. To generate the *AtVHA-c5:GUS* construct, 1.1 kb of the *AtVHA-c5* promoter region was amplified using Col-0 genomic DNA and cloned into the *Hind*III/*Bam*HI site of pBI121 vector. The *AtVHA-c1~c5* promoter primers are as follows: c1pro-F (5'-AAGCTTCTTTGGTCCATTACTCGG-3'), c1pro-R (5'-TCTAGAGTCGGAGTTTTGTATCTGAG-3'); c2pro-F (5'-AAGCTTCGCTGTATCATCTGGTTCG-3'), c2pro-R (5'-TCTAGAGGC TCGTCGTCGTTGAGATC-3'); c3pro-F (5'-AAGCTTCACATTCTACTGCACACACAC-3'), c3pro-R (5'-TCTAGACTCTCAGGCGATTCTGGATC-3'); c4pro-F (5'-AAGCTTTGAAGACG TGGAAC-3'), c4pro-R (5'-CCCGGGGCATTATGAAGACGT-3'); c5pro-F (5'-AAGCTTACGT GGAAAGTACGTAAGCTGC-3') and c5pro-R (5'-GGATCCCTTCTCGGATCTCAAAGTTTTG-3').

The constructs were introduced into the *A. tumefaciens* EHA105 strain for *Arabidopsis* transformation. At least five independent transgenic lines for each construct were selected on 1/2×MS media containing 30 µg mL<sup>-1</sup> kanamycin. Seedlings of the T2 generation were subjected to histochemical assays to detect GUS expression. Plant materials were first incubated at 37 °C for 4 h in the staining buffer (100 mM sodium phosphate, pH 7.0, 10 mM EDTA, 0.5 mM K<sub>3</sub>[Fe(CN)<sub>6</sub>], 0.5 mM K<sub>4</sub>[Fe(CN)<sub>6</sub>], 0.1% Triton X-100) supplemented with 0.5 mM 5-bromo-4-

chloro-3-indolyl- $\beta$ -D-glucuronide (X-Gluc). The stained materials were incubated in 70% ethanol overnight to clear chlorophyll from the green tissues, and then kept in 95% ethanol.

#### **Measurement of Na<sup>+</sup> flux using the ~~non-invasive microelectrode technique~~ (NMT)**

The net Na<sup>+</sup> flux in the rhizosphere was measured by NMT with Na<sup>+</sup>-selective microelectrodes. The microelectrodes were mounted on an electrode holder and calibrated in 10 or 50 mM Na<sup>+</sup> before measuring Na<sup>+</sup> flux. Both WT seedlings and transgenic *Arabidopsis* seedlings that overexpressed *PutVHA-c* were exposed to 10 or 50 mM Na<sup>+</sup> for 24 h, and the root segments were immobilized in the measuring solution (0.1 mM KCl, 0.1 mM CaCl<sub>2</sub>, 0.1 mM MgCl<sub>2</sub>, 0.5 mM NaCl, and 0.3 mM MES, pH 5.8) to measure the Na<sup>+</sup> flux. During measurements, the electrodes were moved in a square wave with 20  $\mu$ m amplitudes at a 5-s cycle from 5  $\mu$ m. The potential differences were recorded for 10 min for each sample. Ion flux was calculated using Fick's law of diffusion

$$J = -D \cdot (dc/dx)$$

where  $J$  represents the ion flux in the  $x$ -direction,  $dc/dx$  is the ion concentration gradient, and  $D$  is the ion diffusion constant in a particular medium. Data and image acquisition, preliminary processing, control of the three-dimensional electrode positioner, and stepper-motor-controlled fine focus of the microscope stage were performed using the ASET software, which is a part of the SIET system (the SIET System, BIO-001A, ~~Younger USA Sci. & Tech. Corp., Amherst, MA~~) (Sun *et al.*, 2009). Three-dimensional ionic fluxes were calculated using Mage Flux, which was developed by Yue Xu (<http://xuyue.net/> or <http://www.youngerusa.com/mageflux>).

#### **Transformation of *P. tenuiflora* suspension-cultured cells**

*P. tenuiflora* seeds were grown in modified MS medium (3% sucrose, 0.5 mg mL<sup>-1</sup> proline, 0.5 mg mL<sup>-1</sup> glutamic acid, 2  $\mu$ g mL<sup>-1</sup> 2,4-dichlorophenoxyacetic acid, 1% agar, pH 5.8) and incubated for 14 days at 22°C to induce calli. *P. tenuiflora* calli were suspended and shaken at 200 rpm in liquid modified MS medium, maintained at 22°C in the dark. The *Agrobacterium tumefaciens* strain, EHA105, was transformed with pBI121-PutVHA-c-GFP and cultured at 28°C in LB broth. *A. tumefaciens* cells (500  $\mu$ L of a culture grown to an OD<sub>600</sub> of 0.5) were added to 5 mL of *P. tenuiflora* suspension cells containing 200 mg mL<sup>-1</sup> acetosyringone. The *P. tenuiflora* suspension cells were co-cultivated at 22°C for 3 days. The cells were then collected using

centrifugation at 500g for 2 min, washed five times with MS liquid media containing 200  $\mu\text{g mL}^{-1}$  cefotaxime, and transferred to agar medium containing 200  $\mu\text{g mL}^{-1}$  cefotaxime and 50  $\mu\text{g mL}^{-1}$  kanamycin. The resultant kanamycin-resistant calli were transferred onto new agar medium that contained only 50  $\mu\text{g mL}^{-1}$  kanamycin, and were then resuspended in liquid medium before being examined by fluorescence microscopy using an Axio imager Z2 epifluorescence microscope (Zeiss, Germany).

## References

Sun, J., Chen, S., Dai, S., Wang, R., Li, N., Shen, X., Zhou, X., Lu, C., Zheng, X., Hu, Z., Zhang, Z., Song, J. and Xu, Y. (2009) NaCl-induced alternations of cellular and tissue ion fluxes in roots of salt-resistant and salt-sensitive poplar species. *Plant Physiol* **149**, 1141-1153.

## Supporting information

### **Conserved V-ATPase c subunit plays a role in plant growth by influencing V-ATPase-dependent endosomal trafficking**

Aimin Zhou <sup>1</sup>, Yuanyuan Bu <sup>1</sup>, Tetsuo Takano <sup>2</sup>, Xinxin Zhang <sup>1</sup>, Shengkui Liu <sup>1\*</sup>

<sup>1</sup> *Key Laboratory of Saline-alkali Vegetation Ecology Restoration in Oil Field (SAVER), Ministry of Education, Alkali Soil Natural Environmental Science Center (ASNESC), Northeast Forestry University, Harbin 150040, China*

<sup>2</sup> *Asian Natural Environmental Science Center, The University of Tokyo, Nishitokyo-shi, Tokyo 188-0002, Japan*

\* Corresponding author: Shengkui Liu (email: shengkui@nefu.edu.cn; fax: +86 451 82191394)

The following materials are available in the online version of this article.

## Supplementary Figures and Figure legends

### Figure S1

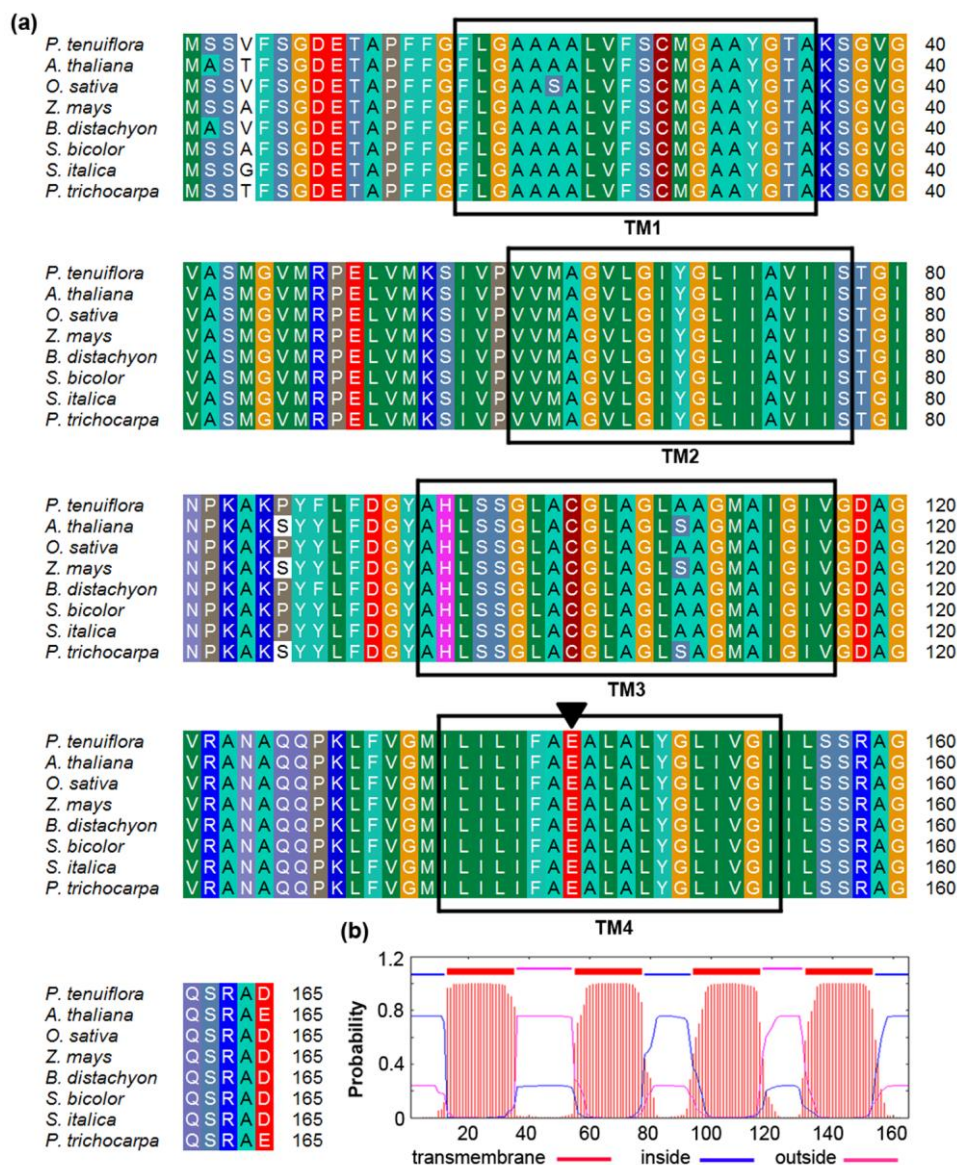


**Figure S1** Sequence alignment of the VHA-c sequences from various plants. (a) Amino acid sequence alignment of PutVHA-c with VHA-c proteins from *Arabidopsis thaliana* (GenBank accession numbers: NP564098), *Oryza sativa* (NP001066258), *Zea mays* (NP001149195), *Brachypodium distachyon* (XP003569121), *Sorghum bicolor* (XP002441892), *Setaria italica* (XP004978799), and *Populus trichocarpa* (XP002307699). Colorized backgrounds indicate identical residues. Black box bars indicate the four putative transmembrane domains. The arrowhead indicates the conserved proton-binding site; (b) Putative transmembrane domains of PutVHA-c. The x-axis indicates the amino acid position.

**Figure S2**

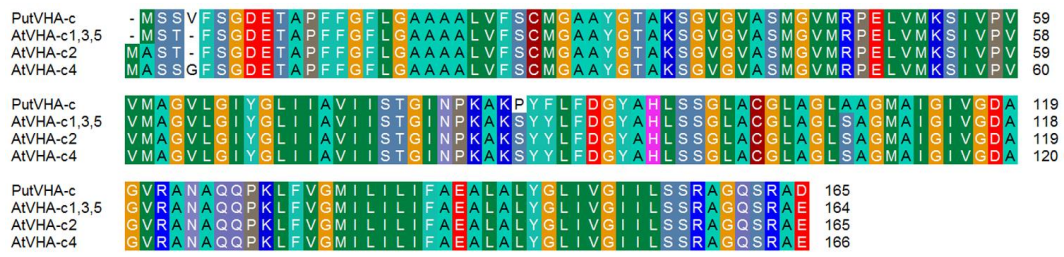


**Figure S2** Alignment of amino acid sequences for PutVHA-c, and three AtVHA-c proteins from *Arabidopsis*. GenBank accession numbers: NP179244, NP564098, and NP 177693. AtVHA-c1, AtVHA-c3 and AtVHA-c5 have the identical sequences, shown here as AtVHA-c1,3,5.

**Figure S3**

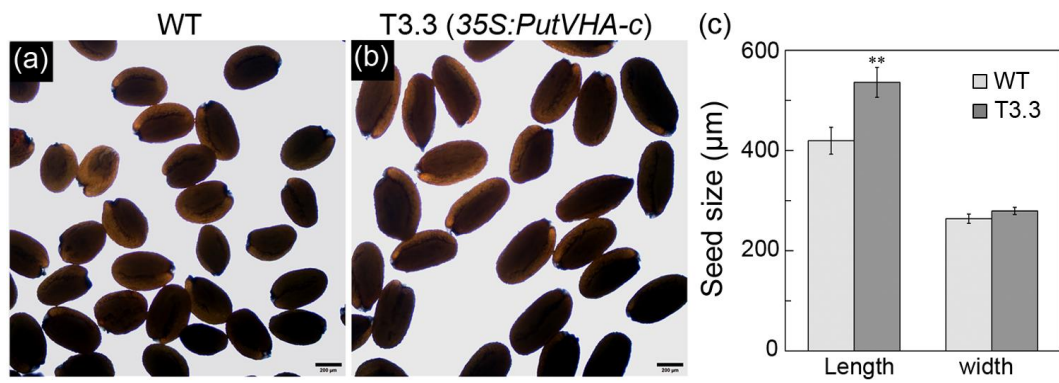


**Figure S3** Seed size comparison of wild-type (WT) and transgenic *Arabidopsis*. (a and b) Appearance (a) and size (b) of WT and transgenic seeds. Error bars represent se ( $n = 50$ ). Asterisks indicate a significant difference between WT and transgenic seeds (\*\* $P < 0.01$ ). Scale bar = 200 µm.

**Figure S4**

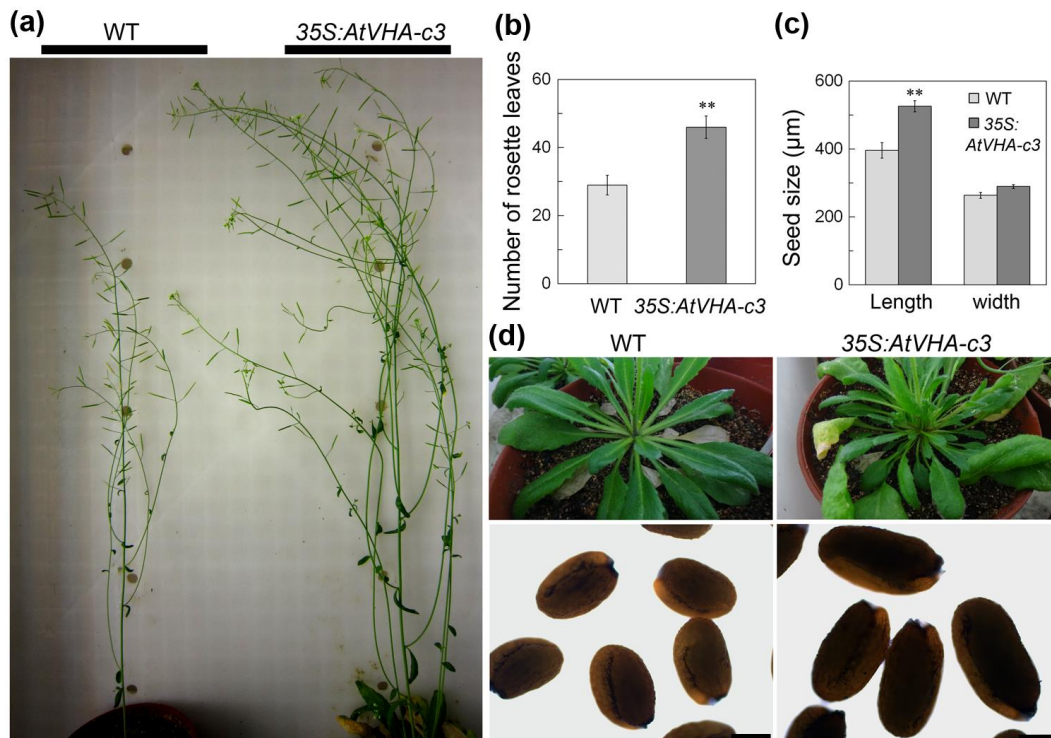


**Figure S4** Phenotypes of wild-type (WT) and transgenic *Arabidopsis* plants overexpressing *AtVHA-c3*. (a) Phenotypes of WT and the transgenic plants grown on soil for 48 days. Seedlings germinated and grown on 1/2 MS medium for 10 days before being transferred to soil; (b–d) The number (b) and phenotypes (d, upper panels) of rosette leaves of WT and transgenic plants grown on soil. Size (c) and appearance (d, lower panels) of seed of WT and transgenic plants. Asterisks indicate a significant difference between WT and transgenic plants ( $*P < 0.05$ ;  $**P < 0.01$ ). Scale bars = 200  $\mu\text{m}$  (d, lower panels).

**Figure S5**

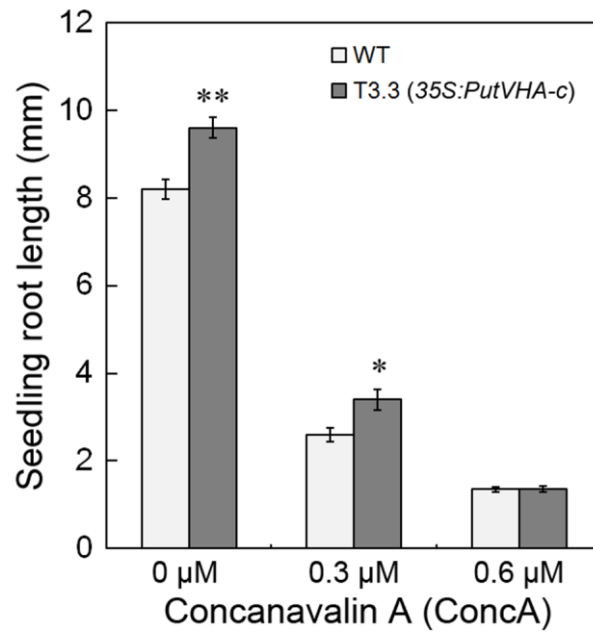


**Figure S5** Concanamycin A (ConcA) affects the root growth of wild-type (WT) and *PutVHA-c* transgenic *Arabidopsis* seedlings. Root lengths of WT and transgenic seedlings (4-day-old) on vertical plates containing 1/2 MS media and the indicated concentrations of ConcA. Error bars represent SE ( $n = 15$ ). Asterisks indicate a significant difference between WT and transgenic seedlings ( $*P < 0.05$ ;  $**P < 0.01$ ). Scale bar = 1 cm.

**Figure S6**

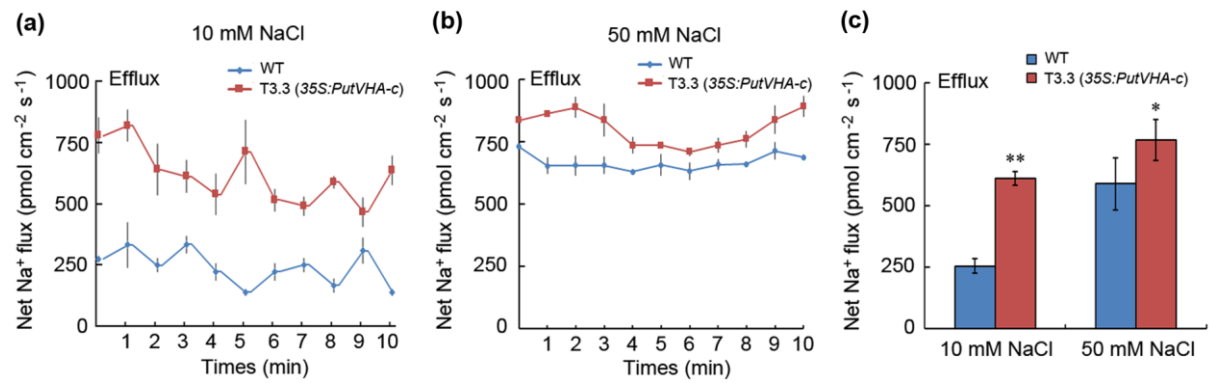


**Figure S6** Net fluxes of Na<sup>+</sup> in the roots of wild-type (WT) and transgenic *Arabidopsis* plants overexpressing *PutVHA-c*. (a and b) Net Na<sup>+</sup> fluxes in 7-day-old seedlings pretreated by 24 h incubation in either 10 (a) or 50 mM (b) NaCl. Continuous flux was recorded for 10 min; (c) Mean Na<sup>+</sup> fluxes from the roots of WT and transgenic seedlings after 24 h incubation in 10 or 50 mM NaCl. Error bars indicate the SE ( $n = 3$ ). Asterisks indicate a significant difference between WT and the transgenic plants (\* $P < 0.05$ ; \*\* $P < 0.01$ ).

**Figure S7**

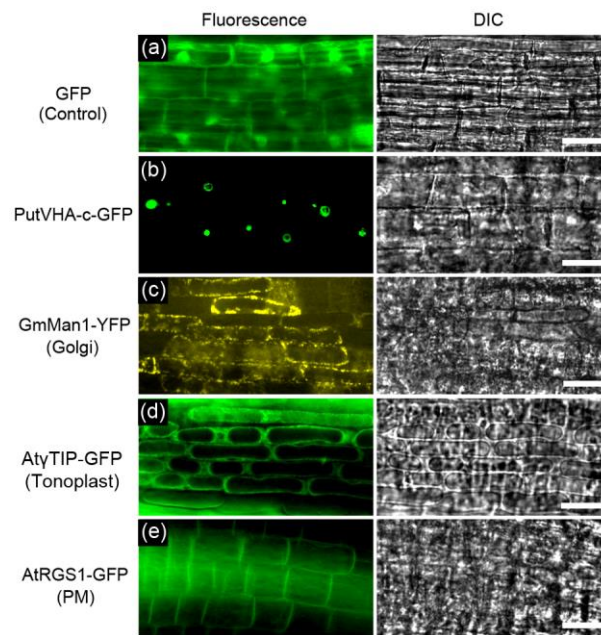


**Figure S7** Comparison of fluorescence patterns of PutVHA-c-GFP and different organelles markers. Confocal images of *Arabidopsis* root cells with the stable expression of GFP alone (a), PutVHA-c-GFP (b), GmMan1-YFP (Golgi) (c), AtγTIP-GFP (tonoplast) (d) and AtRGS1-GFP (plasma membrane) (e). GFP fluorescence is shown in green, YFP fluorescence is shown in yellow. Scale bars = 20  $\mu$ m.

**Figure S8**

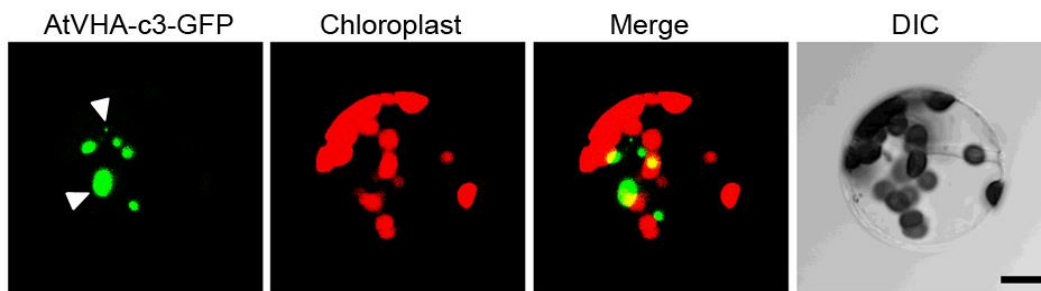


**Figure S8** Confocal images of *Arabidopsis* mesophyll protoplasts with the stable expression of AtVHA-c3-GFP. Arrowheads indicate the punctate structures of different sizes. Solid punctate GFP signals are actually hollow structures in the microscope. Chlorophyll autofluorescence is shown in red. DIC: differential interference contrast. Scale bars = 10  $\mu\text{m}$ .

**Figure S9**

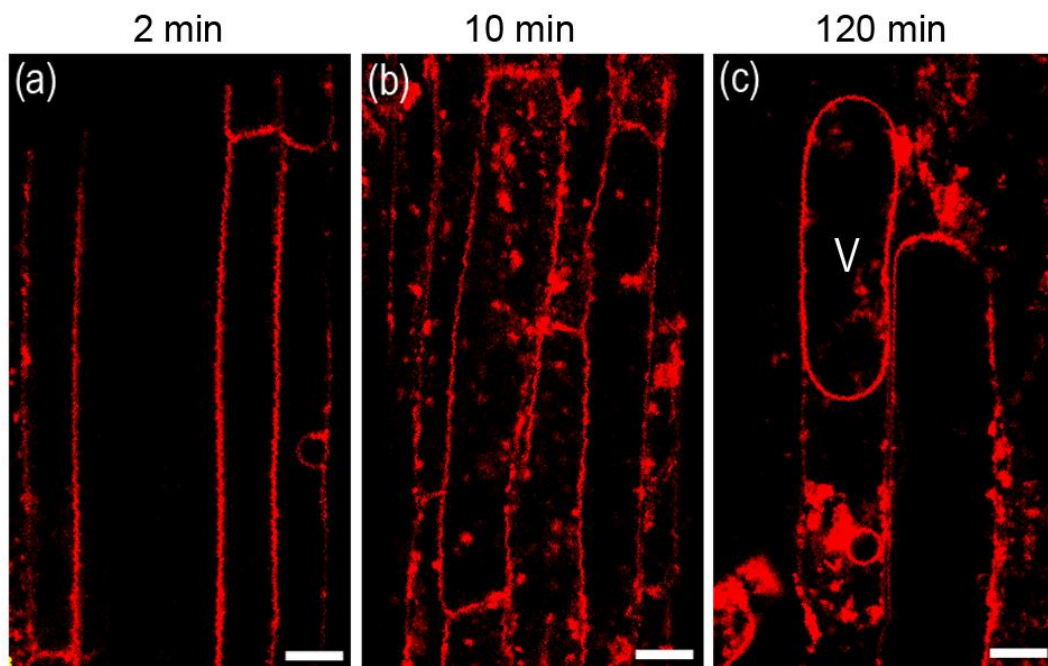


**Figure S9** Time-course of the endosome marker FM4-64 in root cells of *Arabidopsis*. (a–c) Time course of FM4-64 internalization in root epidermal cells, from 2 to 120 min after FM4-64 staining. FM4-64 follows the endocytic pathway, from the plasma membrane (PM) (a) via endosomes (b) to the vacuolar membrane (c). V: vacuole. Scale bars = 10 μm.

**Figure S10**

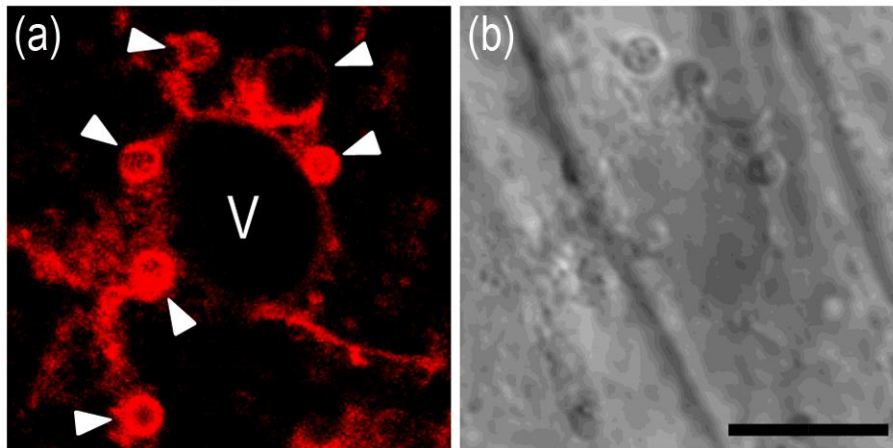


**Figure S10** FM4-64 dye is transported to the vacuole membrane via endosomes. (a) FM4-64 labeled endosomes (arrowheads) and vacuole membrane. (b) Differential interference contrast (DIC) image. Scale bars = 5  $\mu\text{m}$ .

**Figure S11**

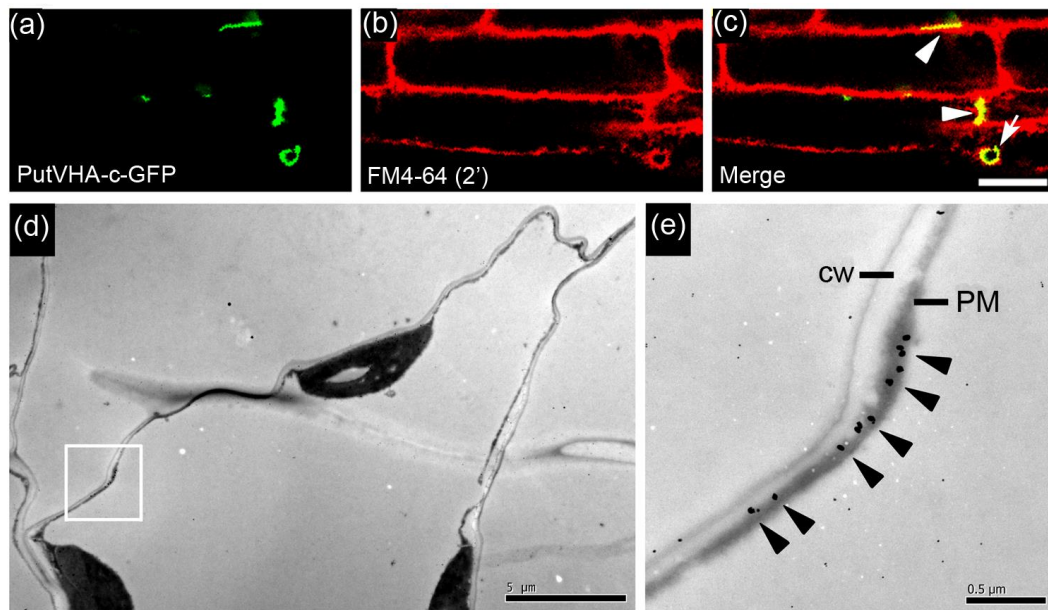


**Figure S11** Localization of PutVHA-c-GFP in *Arabidopsis*. (a–c) Colocalization of PutVHA-c-GFP with membrane structures labeled by FM4-64. Root cells of transgenic *Arabidopsis* plants that express PutVHA-c-GFP (a) 2 min after staining with FM4-64 (b). Arrow indicate the colocalization of PutVHA-c-GFP and FM4-64 on endosome. Arrowheads indicate the colocalization of PutVHA-c-GFP and FM4-64 at parts of the PM (c); (d and e) Immunogold labeling of PutVHA-c-GFP in a leaf from a transgenic *Arabidopsis* plant; (e) Higher magnification of the boxed area in the panel (d). Gold particles were detected in part of the PM (e). PM, plasma membrane; cw, cell wall. Scale bars = 10  $\mu\text{m}$  (a–c), 5  $\mu\text{m}$  (d), 0.5  $\mu\text{m}$  (e).